

# A DYNAMIC ADDITIVE AND MULTIPLICATIVE EFFECTS NETWORK MODEL WITH APPLICATION TO THE UNITED NATIONS VOTING BEHAVIORS \*

BY BOMIN KIM<sup>1</sup>, XIAOYUE NIU<sup>2</sup>, DAVID HUNTER<sup>2</sup> AND XUN CAO<sup>2</sup>

<sup>1</sup>*Freddie Mac*

<sup>2</sup>*The Pennsylvania State University*

Motivated by a study of United Nations voting behaviors, we introduce a regression model for a series of networks that are correlated over time. Our model is a dynamic extension of the additive and multiplicative effects network model (AMEN) of Hoff (2021). In addition to incorporating a temporal structure, the model accommodates two types of missing data thus allows the size of the network to vary over time. We demonstrate via simulations the necessity of various components of the model. We apply the model to the United Nations General Assembly voting data from 1983 to 2014 (Voeten, 2013) to answer interesting research questions regarding international voting behaviors. In addition to finding important factors that could explain the voting behaviors, the model-estimated additive effects, multiplicative effects, and their movements reveal meaningful foreign policy positions and alliances of various countries.

**1. Introduction.** The United Nations was founded in 1945 and today it includes as members nearly all of the world's sovereign states. Each UN member state is also a member of the United Nations General Assembly (UNGA), the main deliberative body of the UN, and each is eligible to vote on matters that come before the UNGA. The votes of the member states reveal much about various states' stances towards each other and on various issues, which helps to understand past foreign policies and state behaviors and predict those yet to come. As such, these votes have been analyzed in many political science papers (see, e.g., Voeten, 2013, and the references therein) and have become standard data sources to study states' preferences, one of the most important topics in the field of international relations.

This article combines and extends statistical ideas to create a novel methodology, then applies this methodology to the UNGA voting data in three innovative ways. First, we consider voting behavior to be dyadic, that is, we explicitly model the similarity and differences in nations' pairs of votes by expressing the voting data in the form of a network dataset that captures the degree to which pairs of nations agree in their votes. Other researchers have viewed UN voting as dyadic behavior and have thus used dyadic similarity indicators such as affinity or S scores (e.g., Gartzke, 1998; Signorino and Ritter, 1999), but to our knowledge, the United Nations voting data have never been analyzed using modern statistical network models. Second, we explicitly model the time dependence of voting agreement. Votes are of course highly correlated over time, because they are the reflections of history. Our model allows for more general temporal dependence than the methods that have previously attempted to account for this dependence using a Markovian assumption (e.g., the dynamic ordinal spatial item response theory model of Bailey et al., 2017) whereby temporal dependence lasts a single time step, i.e., one year. Third, by considering voting patterns as a network dataset in

---

\*This work was supported by the National Institute of Allergy and Infectious Diseases of the National Institutes of Health under award number R01AI136664.

*Keywords and phrases:* Latent space model, varying number of nodes, international policy.

which each nation state is assumed to occupy a position in latent space that may evolve over time, our methodology allows the analysis of high-order dependences such as transitivity and stochastic equivalence. This allows us to consider the fact that voting decisions are not limited to dyadic relations—country A’s decision to vote along with country B might well be influenced by country C’s decision.

We refer to our modeling framework as the dynamic additive and multiplicative effects (DAME) model, since we take as its basis the additive and multiplicative effects (AME) framework of Hoff (2021). We extend the AME framework to handle time-varying networks using Gaussian process dependence structure to arrive at DAME. Our model allows for different forms of the Gaussian process covariance structure, whose length scale we estimate from the data, as well as various types of missing data. In Section 2, we introduce the DAME model, derive the sampling distribution for Bayesian inference, and describe the treatment of missing data. Then we present simulation studies to show the necessity of various components in the DAME model. And in Section 4 we apply the DAME model to the United Nations General Assembly voting network, demonstrate the validity of the model, and discuss the findings.

**2. Dynamic Additive and Multiplicative Effects Model.** Networks can be used to describe relationships among subjects—in this case, members of the UN—by representing the subjects as the nodes of a network and the relationships as the edges of the network. In some contexts, the relationship might be binary, as the presence of political alliances between country A and country B, or directed, as the indicator that country A initiated a conflict with country B. In the current context, we consider a particular relationship that is quantitative and undirected, namely, the voting agreement between pairs of countries.

There has been a lot of work in developing statistical models for networks. With this development, along with the increasing availability of network data, there has been a growing need and capability to model networks that change over time. Some models are intrinsically dynamic in nature, such as the stochastic actor-oriented models originated by Snijders (2001) and developed in subsequent articles (e.g., Snijders et al., 2010) that envision ties as random processes that evolve in time. Other work involves extensions of static network models into the time-varying domain. For instance, the sizable literature on exponential-family random graph models (ERGMs) (see, e.g., Lusher et al., 2013) has been extended by papers such as Hanneke et al. (2010) and Krivitsky and Handcock (2014) to handle discrete-time time-varying networks in which a network at time  $t + 1$  depends explicitly on the network at time  $t$  via one or more statistics measured on the network.

One of the features of social networks and in general human behaviors is that we cannot observe all factors that determine the behaviors. Latent variables help capture this feature and are very common in social science models. An important subset of the statistical networks literature, to which the current article belongs, involves latent variables, i.e., unobserved properties of the network. Kim et al. (2018) provide a comprehensive review of the literature on dynamic network models with latent variables, and more recent development includes Olivella et al. (2022). Here, we consider one type of the latent variable models, i.e. the latent space models, which include distance and projection models (Hoff et al., 2002), the bilinear effects model (Hoff, 2005), and the additive and multiplicative effects model (AME) (Hoff, 2021). While there exist dynamic extensions of the latent distance model and bilinear effects model, to the best of our knowledge, the AME model has not been extended to the dynamic case, which is our focus in this article.

Another challenge in dynamic network modeling is missing data, including missing edges and missing nodes over time. Common practices for handling missing data are to use only the subset of nodes that have complete observations or to treat all missing data as missing

at random and then imputing values to complete the dataset. It is not uncommon for some countries' voting patterns to be disrupted by specific geopolitical factors that may persist over multiple years, so missing data should be treated carefully so as not to inadvertently introduce biases by assuming that such missingness occurs haphazardly. We argue in Section 2.3 that some of the missing mechanisms might not be missing at random, particularly those involving nodes missing for a stretch of time. We therefore propose novel treatments for different missing mechanisms.

2.1. *Extending the AME framework.* This article extends the Gaussian additive and multiplicative effects (AME) framework of Hoff (2021). Since the dataset we study in this paper involves a symmetric network, our starting point is the symmetric AME, which assumes

$$(1) \quad Y_{ij} = \sum_{p=1}^P X_{ijp} \beta_p + a_i + a_j + \mathbf{u}'_i \mathbf{D} \mathbf{u}_j + \epsilon_{ij},$$

where  $Y_{ij}$  is the  $(ij)$ th entry of the sociomatrix ( $\mathbf{Y}_{n \times n}$ ) of the network;  $\boldsymbol{\beta} = (\beta_1, \dots, \beta_P)$  is the  $P$ -length coefficient vector of predictor ( $\mathbf{X}_{n \times n \times P}$ ) effects (including the intercept);  $a_i$  and  $a_j$  are the nodal additive effects, which can be interpreted as each node's "sociability" or "popularity";  $\mathbf{u}_i$  and  $\mathbf{u}_j$  are the  $R$ -dimensional latent factors for nodes  $i$  and  $j$ ; and  $\mathbf{D}$  is an  $R \times R$  diagonal matrix, and finally  $\epsilon_{ij}$  are random errors that are not captured by the previous terms. The asymmetric version of AME can be extended in a similar fashion, as we discuss in Section 5. The multiplicative effect  $\mathbf{u}'_i \mathbf{D} \mathbf{u}_j$  represents the similarity between node  $i$  and node  $j$ , and in this expression the signs of the entries of  $\mathbf{D}$  have important substantive implications: Positive and negative entries indicate homophily and anti-homophily, respectively, with regard to the corresponding dimension in the latent  $\mathbf{u}$  vectors. That is, when nodes  $i$  and  $j$  have values of  $u_{ir}$  and  $u_{jr}$  that are large in magnitude and have matching signs, then the value of the corresponding diagonal element  $d_r$  of  $\mathbf{D}$  determines whether this  $r$ th dimension contributes a positive or negative value to the mean of  $Y_{ij}$ . A positive value corresponds to homophily, whereas a negative value corresponds to anti-homophily.

In extending the symmetric AME model to the time-varying domain, we adapt an idea of Durante and Dunson (2014) by assuming a Gaussian process on the time-varying components. This approach allows for long-term dependence, unlike any model employing a Markovian assumption, since we know that countries' behaviors towards one another fall into patterns that do not change dramatically from year to year. Durante and Dunson (2014) extends a simplified version of Model (1) in which  $\mathbf{u}'_i \mathbf{u}_j$  is used in place of  $\mathbf{u}'_i \mathbf{D} \mathbf{u}_j$ . As discussed above, the  $\mathbf{D}$  matrix allows flexibility in modeling both homophily and anti-homophily, and we further demonstrate in Section 3 the necessity of including  $\mathbf{D}$  in symmetric relational data.

Our dynamic additive and multiplicative effects (DAME) model assumes that for  $1 \leq j < i \leq N$ ,  $1 \leq t \leq T$ ,  $1 \leq p \leq P$ , and  $1 \leq r \leq R$ ,

$$(2) \quad Y_{ij}^t = \sum_{p=1}^P X_{ijp}^t \beta_p^t + a_i^t + a_j^t + \mathbf{u}'_i{}^t \mathbf{D}^t \mathbf{u}_j^t + \epsilon_{ij}^t,$$

$$\boldsymbol{\beta}_p = (\beta_p^1, \dots, \beta_p^T) \sim \mathcal{N}_T(\mathbf{0}, \Sigma_p^\beta) \text{ with } \Sigma_p^\beta(t, t') = \tau_p^\beta f(\kappa_p^\beta, t, t'),$$

$$\mathbf{a}_i = (a_i^1, \dots, a_i^T) \sim \mathcal{N}_T(\mathbf{0}, \Sigma^a) \text{ with } \Sigma^a(t, t') = \tau^a f(\kappa^a, t, t'),$$

$$\mathbf{u}_{ir} = (u_{ir}^1, \dots, u_{ir}^T) \sim \mathcal{N}_T(\mathbf{0}, \Sigma_r^u) \text{ with } \Sigma_r^u(t, t') = \tau_r^u f(\kappa_r^u, t, t'),$$

$$\epsilon_{ij}^t \sim \text{i.i.d. } \mathcal{N}(0, \sigma_e^2).$$

To model the covariance matrices  $\Sigma_1^\beta, \dots, \Sigma_P^\beta$ ,  $\Sigma^a$ , and  $\Sigma_1^u, \dots, \Sigma_R^u$ , we consider two of the commonly used covariance functions (Rasmussen, 2003), the standard exponential, or Ornstein-Uhlenbeck, function and the squared exponential function. The standard exponential function has the form

$$f(\kappa, t, t') = \exp\left(-\frac{|t - t'|}{\kappa}\right),$$

for time points  $t$  and  $t'$ . Replacing the distance term by  $|t - t'|^2$  gives the squared exponential function. When the time intervals are moderately spaced, we would prefer the standard exponential function. On the other hand, if the time interval is very small or smoothness is expected, the squared form is preferred.

We assume independent standard normal priors for the diagonal entries of  $\mathbf{D}$  for the sake of identifiability. Whereas Durante and Dunson (2014) fix the parameter  $\kappa$  that characterizes the length-scale of the process, in practice we may not have prior knowledge about how strongly networks are correlated over time. Thus, we choose to estimate  $\tau$  and  $\kappa$ , and the other parameters with the following prior distributions:

$$\begin{aligned} \tau_p^\beta &\sim \mathcal{IG}(k_\beta, \theta_\beta) \text{ and } \kappa_p^\beta \sim \text{half-Cauchy}(\gamma_\beta) \text{ for } p = 1, \dots, P, \\ \tau^a &\sim \mathcal{IG}(k_a, \theta_a) \text{ and } \kappa^a \sim \text{half-Cauchy}(\gamma_a), \\ \tau_r^u &\sim \mathcal{IG}(k_u, \theta_u) \text{ and } \kappa_r^u \sim \text{half-Cauchy}(\gamma_u) \text{ for } r = 1, \dots, R, \\ d_r^t &\sim \text{i.i.d. } \mathcal{N}(0, 1), \\ \sigma_e^2 &\sim \mathcal{IG}(k_\sigma, \theta_\sigma). \end{aligned}$$

The inverse-Gamma is the most common prior distribution for the variance parameter. The half-Cauchy prior is recommended by Gelman (2006). We experiment different sets of  $(k, \theta)$  and  $\gamma$ , including the g-prior (Zellner (1986)). The final results are all similar but the mixing performances differ slightly. In the end, we choose  $(k, \theta) = (2, 1)$  and  $\gamma = 5$  so that they are weakly informative with the expected value of the variance parameter being 1.

All of the model parameters have clear interpretation and capture various features of the network. Regression coefficients  $\beta$  explain the global features as well as observed covariate (nodal and dyadic) effects of the network. Additive effects  $\mathbf{a}$  describe the across-row and across-column heterogeneities, which are the same thing in the symmetric case. Its variance  $\tau^a$  measures the strength of the dependence induced by sharing the same sender/receiver. Multiplicative factors  $\mathbf{u}$  capture the non-additive, higher order dependence that generates homophily (a social preference to be friends with others similar to you), transitivity (a social preference to be friends with your friends' friends), balance (a social preference to be friends with your enemies' enemies), and stochastic equivalence (similar nodes have similar relational patterns, not necessarily connected to each other). Non-Gaussian data can be dealt with by choosing an appropriate link function in a similar manner as generalized linear models.

**2.2. Bayesian Estimation.** Our posterior computation is performed via a Gibbs sampler to update the vector of time-varying regression coefficients and the vector of additive and multiplicative latent factors, along with a Metropolis-Hastings (MH) algorithm to sample the variance and length GP parameters  $(\tau, \kappa)$ . Full conditional distributions and details about the MH algorithm are provided in Supplementary Materials Sections A and B (Kim et al. (2023)).

Let  $\mathbf{E}^t$  denote the  $N \times N$  matrix of random noise, where the  $(i, j)^{th}$  entry is defined as

$$E_{ij}^t = y_{ij}^t - \sum_{p=1}^P X_{ijp}^t \beta_p^t - a_i^t - a_j^t - \mathbf{u}_i^{t'} \mathbf{D}^t \mathbf{u}_j^t.$$

Given that the distribution of the observed network  $\mathbf{Y} = \{\mathbf{Y}^1, \dots, \mathbf{Y}^T\}$  conditional on all the parameters can be written as the product of Normal probability density functions as

$$\begin{aligned} & \text{Pr}(\mathbf{Y} | \mathbf{X}, \boldsymbol{\beta}, \mathbf{a}, \mathbf{d}, \mathbf{u}, \sigma_e^2, \boldsymbol{\tau}^\beta, \boldsymbol{\tau}^a, \boldsymbol{\tau}^d, \boldsymbol{\tau}^u, \boldsymbol{\kappa}^\beta, \boldsymbol{\kappa}^a, \boldsymbol{\kappa}^u) \\ (3) \quad & \propto \prod_{t=1}^T \prod_{i>j} (\sigma_e^2)^{-\frac{1}{2}} \exp \left\{ -\frac{1}{2\sigma_e^2} \|E_{ij}^t\|^2 \right\}, \end{aligned}$$

we sequentially update each parameter from its full conditional distribution in the following sampling steps:

1. Sample  $\sigma_e^2 \sim \mathcal{IG}\left(\frac{T \cdot N(N-1)}{4} + k_\sigma, \frac{1}{2} \sum_{t=1}^T \sum_{i>j} (E_{ij}^t)^2 + \theta_\sigma\right)$ .
2. For each  $p = 1, \dots, P$  in a random order, sample  $\boldsymbol{\beta}_p$  as follows:
  - a) Sample  $(\tau_p^\beta, \kappa_p^\beta)$  using the MH algorithm of Supplementary Materials Section B (Kim et al. (2023)).
  - b) Sample  $\boldsymbol{\beta}_p \sim \mathcal{N}_T(\tilde{\mu}_{\beta_p}, \tilde{\Sigma}_{\beta_p})$  with

$$\tilde{\Sigma}_{\beta_p} = \left( (\Sigma_p^\beta)^{-1} + \frac{\text{diag}(\{\sum_{i>j} X_{ijp}^{t2}\}_{t=1}^T)}{\sigma_e^2} \right)^{-1} \quad \text{and} \quad \tilde{\mu}_{\beta_p} = \left( \frac{\{\sum_{i>j} (E_{ij[-p]}^t X_{ijp}^t)\}_{t=1}^T}{\sigma_e^2} \right) \tilde{\Sigma}_{\beta_p},$$

where  $E_{ij[-p]}^t = E_{ij}^t + \beta_p^t X_{ijp}^t$  and  $\Sigma_p^\beta = \tau_p^\beta f(\kappa_p^\beta)$ .

3. Sample  $\mathbf{a}_i$  as follows:
  - a) Sample  $(\tau^a, \kappa^a)$  using the MH algorithm of Supplementary Materials Section B (Kim et al. (2023)).
  - b) For each  $i = 1, \dots, N$  in a random order, sample  $\mathbf{a}_i \sim \mathcal{N}_T(\tilde{\mu}_{a_i}, \tilde{\Sigma}_{a_i})$  with

$$\tilde{\Sigma}_{a_i} = \left( (\Sigma_a)^{-1} + \frac{(N-1)I_T}{\sigma_e^2} \right)^{-1} \quad \text{and} \quad \tilde{\mu}_{a_i} = \left( \frac{\{\sum_{j \neq i} E_{ij[-i]}^t\}_{t=1}^T}{\sigma_e^2} \right) \tilde{\Sigma}_{a_i},$$

where  $E_{ij[-i]}^t = E_{ij}^t + a_i^t$ ,  $\Sigma^a = \tau^a f(\kappa^a)$ .

4. For each  $r = 1, \dots, R$  in a random order, sample  $\mathbf{u}_{ir}$  as follows:
  - a) Sample  $(\tau_r^u, \kappa_r^u)$  using the MH algorithm of Supplementary Materials Section B (Kim et al. (2023)).
  - b) For  $i = 1, \dots, N$  in a random order, sample  $\mathbf{u}_{ir} \sim \mathcal{N}_T(\tilde{\mu}_{u_{ir}}, \tilde{\Sigma}_{u_{ir}})$  with

$$\tilde{\Sigma}_{u_{ir}} = \left( (\Sigma_r^u)^{-1} + \frac{\text{diag}(\{\sum_{j \neq i} (d_r^t u_{jr}^t)^2\}_{t=1}^T)}{2\sigma_e^2} \right)^{-1} \quad \text{and} \quad \tilde{\mu}_{u_{ir}} = \left( \frac{\{\sum_{j \neq i} (E_{ij[-r]}^t d_r^t u_{jr}^t)\}_{t=1}^T}{2\sigma_e^2} \right) \tilde{\Sigma}_{u_{ir}},$$

where  $E_{ij[-r]}^t = E_{ij}^t + u_{ir}^t d_r^t u_{jr}^t$  and  $\Sigma_r^u = \tau_r^u f(\kappa_r^u)$ .

5. For each  $r = 1, \dots, R$  in a random order, sample  $\mathbf{d}_r$  as follows:
  - (a) Sample  $\mathbf{d}_r \sim \mathcal{N}_T(\tilde{\mu}_{d_r}, \tilde{\Sigma}_{d_r})$  with

$$\tilde{\Sigma}_{d_r} = \left( I_T + \frac{\text{diag}(\{\sum_{i>j} (u_{ir}^t u_{jr}^t)^2\}_{t=1}^T)}{\sigma_e^2} \right)^{-1} \quad \text{and} \quad \tilde{\mu}_{d_r} = \left( \frac{\{\sum_{i>j} (E_{ij[-r]}^t u_{ir}^t u_{jr}^t)\}_{t=1}^T}{\sigma_e^2} \right) \tilde{\Sigma}_{d_r},$$

where  $E_{ij[-r]}^t = E_{ij}^t + u_{ir}^t d_r^t u_{jr}^t$ .

Note that after steps 2 through 5,  $\mathbf{E} = \{\mathbf{E}^1, \dots, \mathbf{E}^T\}$  has to be calculated again using the previously updated values, so that any update is conditioned on the current values of all the other parameters.

**2.3. Missing Data.** In dynamic networks, nodes or edges can be missing at any time point. One method to handle such missing data is to use the network consisting only of the completely observed set of nodes, though we avoid this idea because it might lead to loss of information and potentially biased estimates. Another idea (e.g., [Sewell and Chen, 2015](#)) is to treat all missing data as missing at random and impute them. However, in our application, the specific reason for a missing data point is sometimes known, as for instance in the case of a nation state that did not exist prior to a certain year and therefore joined the UN later than other states. Moreover, if we have covariates in the data, these covariates might have different relationships with the missing nodes than with the observed nodes. For these reasons, imputation of all missing edge data might generate biases.

To address missing data in our application, therefore, we define two types of missing data—“random missing” and “structural missing”. Let  $N$  denote the number of nodes that are part of the network at any time from 1 to  $T$ , then define the  $N \times T$  node availability matrix  $\mathbf{A}$  so that  $A_{nt}$  equals 1 or 0, depending on whether or not node  $n$  is available, i.e., non-missing, at time  $t$ , respectively. Without prior knowledge on the missing mechanism, we assume that missing edges corresponding to node  $n$  at time  $t$  for which  $A_{nt} = 1$  are random missing, while those for which  $A_{nt} = 0$  are structural missing. Random missing edges are imputed from the current parameter estimates at each MCMC iteration, while structural missing edges are excluded from the likelihood and the parameters are estimated without them. This procedure is beneficial even if the model does not contain covariates, since imputing values that are not missing at random could bias the temporal correlation estimates of additive and/or multiplicative effects.

**3. Simulation Study.** Our simulation study has two objectives: First, to show that estimation of the correct covariance structure plays a key role in the model performance, particularly in the case of modeling a network that is highly correlated across time; and second, to demonstrate that the eigen-decomposition formulation of the multiplicative random effects ( $\mathbf{u}'\mathbf{D}\mathbf{u}$ ) clarifies various transitivity effects.

**3.1. Estimating Temporal Correlations.** We simulate three dynamic network datasets according to the generative process in Section 2.1, with  $N = 20$ ,  $T = 10$ ,  $P = 1$  (intercept-only),  $R = 2$ , and  $(k, \theta) = (2, 1)$  for all  $\tau$  parameters as well as  $\sigma_e^2$ . We use the standard exponential covariance function with three different levels of correlation: High ( $\kappa = 30$ ), medium ( $\kappa = 2$ ), and low ( $\kappa = 0.001$ ). For each generated dataset, we fit the DAME model both while estimating  $\kappa$  and while holding  $\kappa$  fixed at an incorrect value.

We define the “lag-1 degree correlation” statistic as the Pearson correlation  $\rho(\cdot)$  between the vectors  $v_1 = [\text{deg}(\mathbf{Y}^1), \dots, \text{deg}(\mathbf{Y}^{T-1})]$  and  $v_2 = [\text{deg}(\mathbf{Y}^2), \dots, \text{deg}(\mathbf{Y}^T)]$ , where  $\text{deg}(\mathbf{Y}^t)$  is defined as the  $N$ -dimensional row vector whose entries are the degree statistics for all nodes. That is,  $\text{deg}(\mathbf{Y}^t) = (\sum_{j=1}^N y_{1j}^t, \sum_{j=1}^N y_{2j}^t, \dots, \sum_{j=1}^N y_{Nj}^t)$ .

For all three parameter settings, we run 48,000 MCMC iterations, which appears to be enough for convergence, calculating the lag-1 degree correlation statistic for a randomly generated posterior predicted  $\mathbf{Y}$  at each iteration. In Figure 1, we present the results after discarding the first 8,000 samples and using a thinning interval of 20. For the high correlation case (left),  $\kappa$  is fixed at 2 and 0.001 to represent misspecifying at medium and low values. For the medium correlation case (middle),  $\kappa$  is fixed at 30 and 0.001 to represent misspecifying at high and low values. For the low correlation case (right),  $\kappa$  is fixed at 30 and 2 to represent

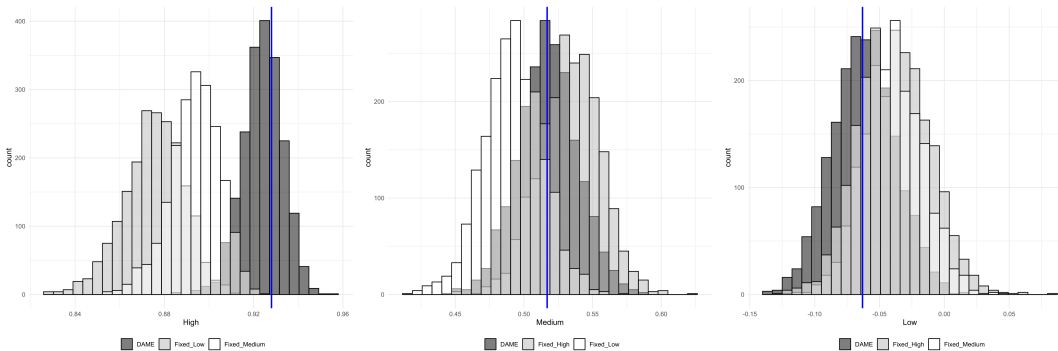


FIGURE 1. Posterior distributions of lag-1 degree correlations. The temporal correlations use the standard exponential covariance function with  $\kappa = 30$  (left),  $\kappa = 2$  (middle), and  $\kappa = 0.001$  (right). The vertical line in each plot represents the true value of the lag-1 degree correlation.

misspecifying at high and medium values. The true correlation is represented by the vertical line in each plot. The plots show that posterior distributions of the lag-1 degree correlation center around the wrong values when  $\kappa$  is misspecified, while the full DAME model can correctly recover this correlation. This suggests that in the absence of prior information about the temporal correlation of the network, it is wise to estimate  $\kappa$  from the data.

**3.2. Estimating Homophily and Transitivity.** As explained in Section 2.1, The  $\mathbf{D}^t$  term in Equation (2) helps capture both homophily and anti-homophily effects. As explained for example by Goodreau et al. (2009), these homophily effects can operate between actors, in this case nation states, to produce higher order global effects such as transitivity. We illustrate this phenomenon via a different simulation study.

As in Section 3.1, we take  $N = 20$ ,  $T = 10$ ,  $P = 1$  (intercept-only),  $R = 2$ , and  $(k, \theta) = (2, 1)$  for all  $\tau$  parameters as well as  $\sigma_e^2$ , and simulate model parameters from their respective prior distributions. We use three sets of homophily effects: First, we take  $d_1^t = d_2^t = 2$ ; second, we take  $d_1^t = -d_2^t = 2$ ; and third, we take  $d_1^t = d_2^t = -2$  for all  $t$ . In each case we fit both the DAME model as well as the simpler model in which  $\mathbf{u}^{t'} \mathbf{D}^t \mathbf{u}^t$  is replaced by  $\mathbf{u}^{t'} \mathbf{u}^t$ . Thus, the model is misspecified in the second and third cases. To isolate the high-order effects we wish to illustrate, we assume that the dynamic networks are independent over time by setting  $(\kappa^\beta, \kappa^a, \kappa^d) = (0, 0, 0)$  and fixing these  $\kappa$  parameters at zero throughout the estimation procedure.

Figure 2 gives posterior statistics resulting from 48,000 MCMC iterations to which we apply a thinning interval of 20 after discarding the first 8,000. The three columns are the statistics  $\text{deg}[\mathbf{Y}^t]$ ,  $\text{deg}[(\mathbf{Y}^t)^2]$ , and  $\text{deg}[(\mathbf{Y}^t)^3]$  for a randomly chosen node, where the  $N$ -dimensional deg operator is defined in Section 3.1 and  $(\mathbf{Y}^t)^2$  and  $(\mathbf{Y}^t)^3$  are the square and cube of the matrix  $\mathbf{Y}^t$ , which represent different orders of moment of the original data and can be viewed as a type of goodness-of-fit statistics.

In the top row, the simpler model using  $\mathbf{u}^{t'} \mathbf{u}^t$  is correct, and we see no difference between the two models' results. Yet in the case of mixed (second row) or negative (third row) transitivity, the two formulations reveal noticeable differences. While the DAME model can still recover the true degrees of the first to third moments, the simpler model cannot generate posterior networks that are close to the data in terms of the degree statistics. Not only does the simpler model introduce bias, but also it yields significantly wider interval estimates, implying lower precision compared to the DAME model. In addition, the evidence of the simpler model's failure to capture the transitivity effects becomes larger as the network tends toward stronger negative transitivity and also as we move to the degree statistics in higher moments.

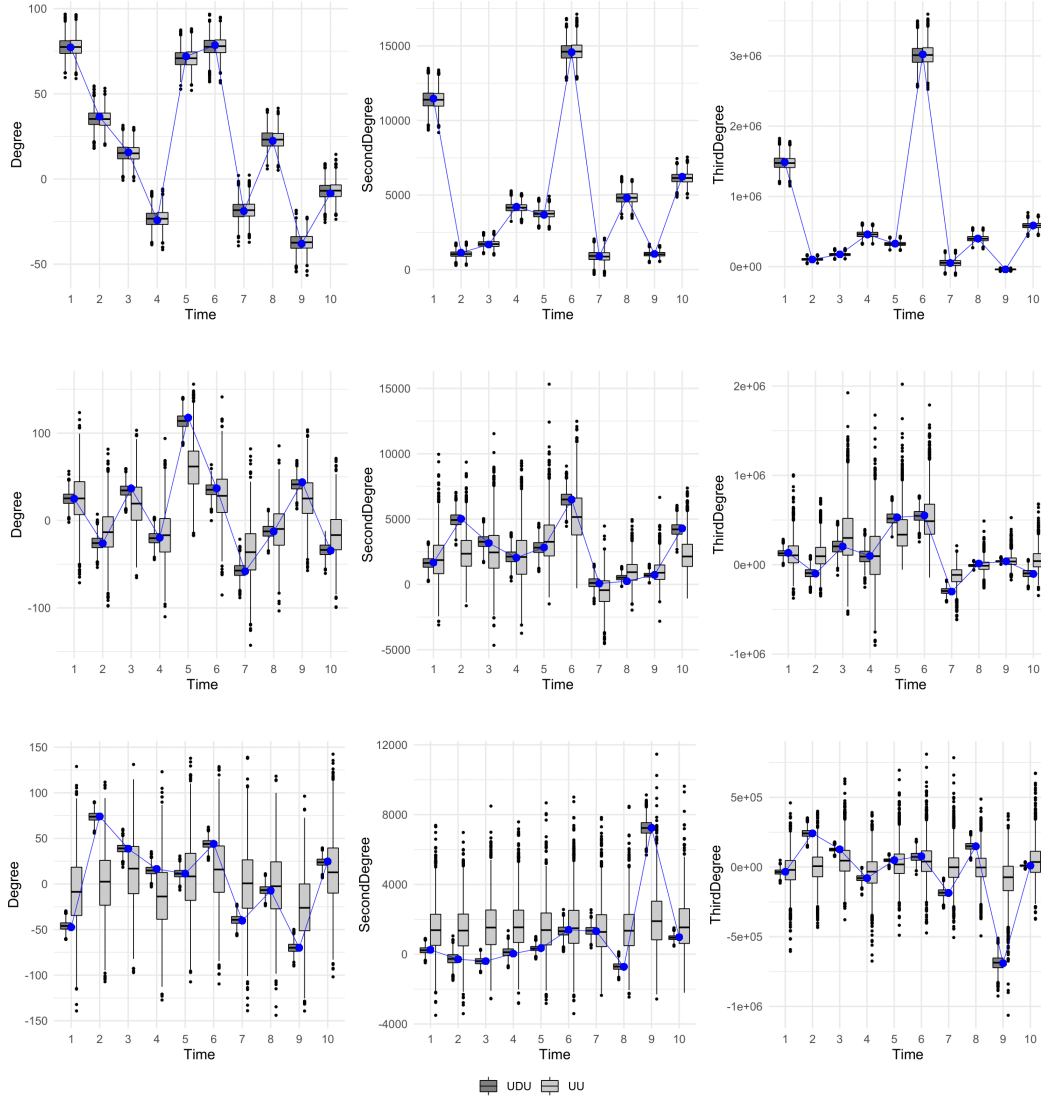


FIGURE 2. Boxplots of 2,000 posterior predictive degree statistics in the first (left), second (center), and third (right) moments corresponding to positive (upper), mixed (middle), and negative (lower) transivities: the DAME and the  $u^u$  models are shown with the connected dots representing the observed statistics.

These findings support our choice of the DAME framework in order to capture high-order effects such as transitivity.

**4. Analysis of the United Nations Voting Network.** States' preferences towards each other and their stances on different issues help us predict future foreign policies and state behaviors, an important topic in the political science literature. Votes in the United Nations General Assembly (UNGA) are a standard data source for studying these preferences, and by considering them as a time-varying network dataset using the novel DAME methodology, we hope to address the following questions:

- What factors are associated with how countries vote? How do those associations change over time?
- Which countries are either more likely or less likely to vote with others? How do those behaviors change over time?

- Beyond observed factors, are there any other unobserved alliances that contribute to countries’ voting behavior? How do those alliances change over time?

The dataset and code used in this section can be found at <https://github.com/bomin8319/DAME>.

4.1. *Data Description.* We consider the time period 1983–2014, which covers important international events such as the Cold War and Iraq War. We first determine the countries to be included in this analysis by the availability of a set of predictors, such as polity score and GDP. We drop countries that have at least one predictor with more than 10 years of missing data. Any remaining missing values are imputed using the data from previous years. The resulting 97 countries are provided along with their abbreviations in Supplementary Materials Section C (Kim et al. (2023)).

The voting data are obtained from Voeten (2013). We use the subset of the votes called “important votes”, identified by the U.S. State Department as “votes on issues which directly affected important United States interests and on which the United States lobbied extensively.” For example, in 2001, important votes include “Israeli Actions in the Occupied Territories,” “Peaceful Settlement of the Question of Palestine,” “U.S. Embargo Against Cuba,” and “Nuclear Disarmament.” Additional information on these data is provided by the U.S. Department of State at <https://www.state.gov/voting-practices-in-the-united-nations/>. The number of important votes ranges from 6 to 28 per year, with an average of 12. Annual voting agreement rates for both important and non-important votes are provided in Supplementary Materials Section D (Kim et al. (2023)).

The voting data could be viewed as a two-mode, or bipartite, network, where one mode is the set of countries and the other is the set of votes. However, since we are primarily interested in relationships between countries in this context rather than any features of the votes themselves, we project the two-mode network to a one-mode network and accept the loss of information that this entails. Each vote has three categories: Y = “yes” or approval of an issue, A = “abstain,” and N = “no” or disapproval of an issue. As we are interested in the relationship of voting agreement between countries, following Voeten (2013), we define an indicator variable  $y_{ijt}^k$  as agreement between each pair of countries on each vote in which they both participate, and define abstain with others as half agreement, i.e.

$$y_{ijt}^k = \begin{cases} 1 & \text{if } i \text{ and } j \text{ vote Y/Y, N/N, or A/A} \\ 0.5 & \text{if } i \text{ and } j \text{ vote Y/A or N/A} \\ 0 & \text{otherwise.} \end{cases}$$

Each vote is on a specific matter, and the relational network constructed from the vote-by-vote data would give us estimates of countries’ voting patterns that jump around reflecting the UN agenda more than countries’ stand. Therefore, instead of the vote-specific agreement, we take the annual average agreement to be our response. Specifically, let  $n_{ij}^t$  denote the number of votes in which both  $i$  and  $j$  participated in year  $t$  and define  $Y_{ij}^t = (\sum_k y_{ijt}^k / n_{ij}^t) \times 100$ . The combined response  $\mathbf{Y} = \{\mathbf{Y}^1, \dots, \mathbf{Y}^{32}\}$  is a  $97 \times 97 \times 32$ -dimensional array representing the percentage of annual agreement and taking values between 0 and 100.

Next, we construct  $P = 6$  covariates from the Correlates of War data (Gibler, 2008), the Polity IV data (Marshall et al., 2014), the International Monetary Fund’s Direction of Trade Statistics, and the International Financial Statistics data. For  $p = 1, \dots, P$ , the explanatory variable  $X_{ijp}^t$  is the following:

1.  $X_{ij1}^t$ : The constant 1, an intercept to account for the baseline degree of agreement.

2.  $X_{ij2}^t$ : distance from gravity model (Ward and Hoff (2007)):  $\log(\text{geographic distance between the capital cities of country } i \text{ and country } j)$ .
3.  $X_{ij3}^t$ : Indicator of whether country  $i$  and country  $j$  have a formal alliance including mutual defense pacts, non-aggression treaties, and ententes at time  $t$ .
4.  $X_{ij4}^t$ : absolute difference in Polity IV score between country  $i$  and country  $j$  at time  $t$ . These scores range from  $-10$  to  $+10$  and provide annual information on the level of democracy, with  $-10$  to  $-6$  corresponding to autocracy,  $-5$  to  $5$  to anocracy, and  $6$  to  $10$  to democracy.
5.  $X_{ij5}^t$ : index of economic dependence using bilateral trade weighted by each country's gross domestic product (GDP), as defined in Gartzke (2000). That is,

$$X_{ij5}^t = \min\left(\frac{\text{Trade}_{ijt}}{\text{GDP}_{it}}, \frac{\text{Trade}_{ijt}}{\text{GDP}_{jt}}\right).$$

6.  $X_{ij6}^t$ : indicator of whether country  $i$  and country  $j$  share the official language.

By definition, all covariates are symmetric, i.e.,  $X_{ijp}^t = X_{jip}^t$ , and all but two of them,  $\log(\text{distance})$  and common language, may vary over time. Correlations between the covariates are summarized in Supplementary Materials Section D (Kim et al. (2023)).

The matrix of availability  $\mathbf{A}$ , introduced in Section 2.3, reflects some countries' non-participation in the United Nations General Assembly (UNGA), as follows:

- North Korea (PRK) and South Korea (ROK) have structural missing values from  $t = 1$  to  $t = 8$  because neither voted until North Korea and South Korea were simultaneously admitted to the United Nations in 1991.
- Russia (RUS) has structural missing values from  $t = 1$  to  $t = 9$  because Russia assumed the Soviet Union's seat, including its permanent membership on the Security Council in the United Nations, after the dissolution of the Soviet Union in 1991.
- Iraq (IRQ) has structural missing values from  $t = 13$  to  $t = 21$  because it did not participate in UNGA roll call votes from 1995 to 2003. Under the rule of Saddam Hussein, Iraq had been under sanctions from the international community, including the UN, since 1990.

As explained in Section 2.3, other missing values are treated as missing at random and thus imputed.

**4.2. Model Validation.** Before interpreting the results of fitting the DAME model, we generate multiple posterior predictive datasets from the fitted model for the purpose of validation. Year by year, we compare the mean and standard deviation of the first-, second-, and third-order moment statistics, as defined in Section 3.2, of the generated datasets to the observed statistics. Figure 3 shows that the model-generated statistics resemble those features of the observed data well. We use  $R = 2$  for the dimension of the latent space of the multiplicative effects in model (2). This choice is based on informally experimenting with several possible choices for  $R$  rather than a formal model selection procedure; we say a bit more about this choice in Section 5.

Finally, we investigate the necessity of including each component in the DAME model. Specifically, we fit four different special cases of the model (2), according to whether the additive effects  $a_i^t + a_j^t$  and/or the multiplicative effects  $\mathbf{u}_i^t \mathbf{D}^t \mathbf{u}_j^t$  are included. Each of the four cases includes the covariate term  $X_{ijp}^t \beta_p^t$ . Figure 4 depicts the degree statistics constructed from 1,000 different posterior predictive samples, where the degrees are normalized for better visibility. Here we take the United States (USA) as an example to discuss the general findings. An alternative figure with the model NO with neither effects are provided in Supplementary Materials Section E (Kim et al. (2023)).

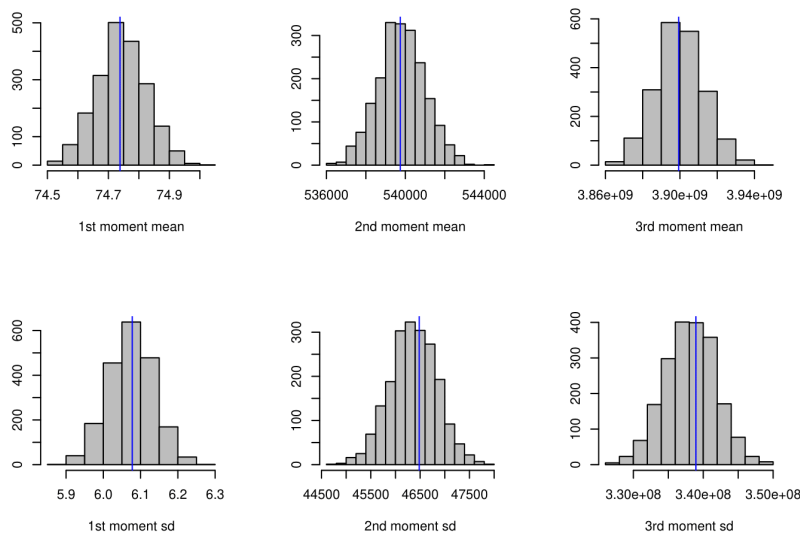


FIGURE 3. *Posterior predictive distribution of the mean and standard deviations of first, second, and third order moment statistics. The observed statistics are represented by the vertical lines.*

Figure 4 shows that inclusion of either the additive effects or the multiplicative effects has the effect of reducing bias, and the AE model has slightly smaller bias than the ME model. Furthermore, the multiplicative effects evidently increase the precision of the estimates. In other words, it appears that the use of both additive and multiplicative effects in the full DAME model achieves both low bias and high precision.

Calculating the sum of squared errors (SSE) of the degree statistics over all 1,000 posterior samples, 97 countries, and 32 time points for each of the four models of Figure 4, where

$$\text{SSE} = \sum_{t=1}^{32} \sum_{k=1}^{1000} \left\| \text{deg}(\mathbf{Y}^t) - \text{deg}(\hat{\mathbf{Y}}_k^t) \right\|^2,$$

we obtain 5.539 for the NO model, 0.148 for AE, 0.035 for ME, and 0.018 for DAME.

In addition, we perform simulation studies to demonstrate the robustness of our model under violations of the normality assumption (Supplementary Materials Section F (Kim et al. (2023))). Goodness of fit plots which evaluate how well the models fit the observed networks based on degree statistics and transitivity property (Hunter et al., 2008) are provided in Supplementary Materials Section G (Kim et al. (2023)).

**4.3. Results and Interpretation.** The results here are based on 150,000 Gibbs iterations. Due to strong autocorrelation among the parameters, we tuned the chain with a burn-in of 50,000 and thinned the iterations by keeping every 50<sup>th</sup> sample.

Figure 5 shows the posterior mean estimates of the fixed effects coefficients  $\{\beta_p\}_{p=1}^P$  with their corresponding 95% credible intervals. Overall, the effects of the covariates on the United Nations voting behavior change substantially over time, especially in the cases of geographic distance and trade-to-GDP ratio. Most importantly, the critical juncture for these temporal changes seems to be around the end of Cold War, that is, the late 1980s and early 1990s. For instance, the middle panel of the top row reveals the pattern of influence of geographic distance on voting behavior. The gravity model (Leibenstein, 1966; Rodrigue et al.,

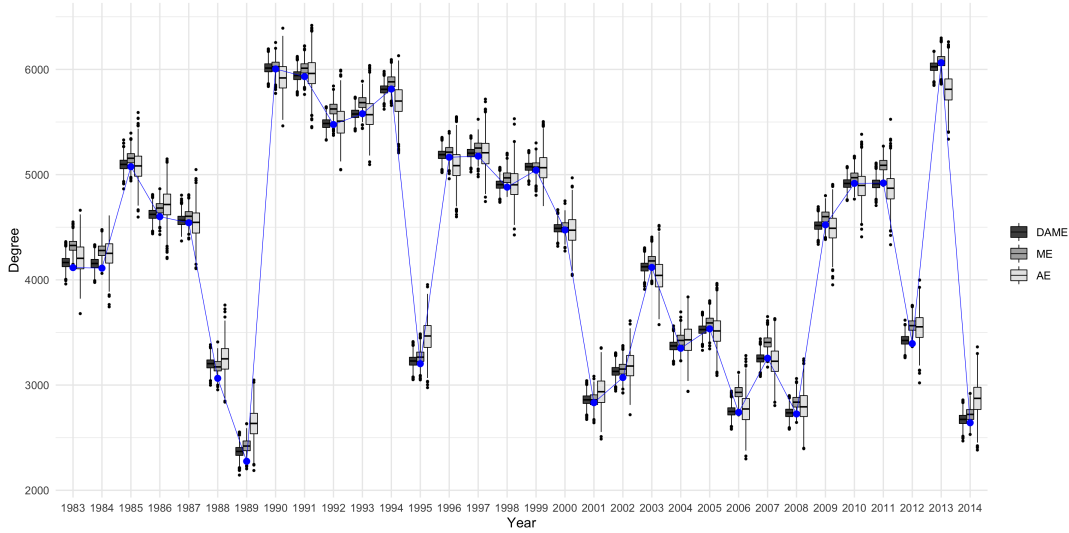


FIGURE 4. Boxplots of 1,000 posterior predictive degree statistics for the United States (USA) for three models: The full DAME with both additive and multiplicative effects, the multiplicative effects only model ME, and the additive effects only model AE. The connected dots show the observed statistics.

2016) suggests that bilateral flows, e.g., trade, migration, or portfolio investment, between two countries are a negative function of the distance between them. We see an overall negative coefficient for geographic distance, which is consistent with the gravity model. However, the negative effect of geographic distance is less significant after the early 1990s. It is likely that the votes in the United Nations were much more influenced by the overall ideological conflicts between the Soviet Union plus its satellites on one side and the Western camp on the other, so the effect of geographical distance was weakened during the Cold War.

Regarding the effect of polity—or distance between polity scores as we operationalize this variable—the result suggests that in general, political regime similarity is not often associated with high agreement in the United Nations General Assembly, at least for a few time periods included in the study, e.g., 1990–1995, 1997–2002, and 2005–2010. Scholars in the liberal tradition of international relations have long argued for shared norms, values, and preferences between democracies; what the result here suggests is that such similarity in preferences is not sufficiently strong to sway countries’ votes in the United Nations General Assembly, at least in the case of important votes and when we account for the other factors in the model. On the other hand, as we expect, having alliances, active trade, and common languages all have positive effects on voting similarity. The posterior mean estimates of  $\kappa$ ’s, the range parameters of Gaussian process, corresponding to the fixed effects are  $\kappa_{intercept}^{\beta} = 68.514$ ,  $\kappa_{\log(distance)}^{\beta} = 4.817$ ,  $\kappa_{polity}^{\beta} = 194.444$ ,  $\kappa_{alliance}^{\beta} = 3.587$ ,  $\kappa_{trade/GDP}^{\beta} = 650.589$ , and  $\kappa_{language}^{\beta} = 3.085$ , which show that these time-varying parameters are correlated over time with long memories.

As for the random effects, for clear visualization we only present the results from 6 countries where 5 are permanent members (China, France, Russia, the United Kingdom, and the United States) and Israel being added based on its large additive random effects. These 6 countries are marked with asterisks in Supplementary Materials Section C (Kim et al. (2023)). Figure 6 shows the posterior mean estimates of each country’s additive random effects, that is, its node-specific time-varying intercepts  $a_i^t$  from Model (2). Here, the United States (USA) and Israel (ISR) stand out with large negative additive random effects, suggesting that these

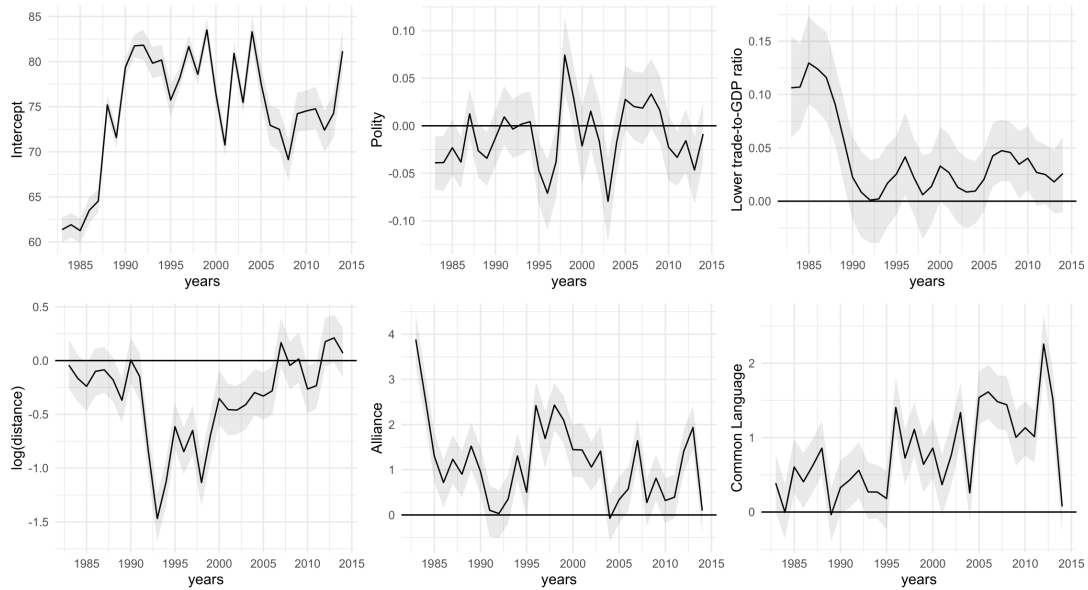


FIGURE 5. Posterior mean estimates (colored lines) and 95% credible intervals (gray areas) for the fixed effect coefficients  $\beta$  corresponding to intercept,  $\log(\text{distance})$ , alliance, polity difference, lower trade-to-GDP ratio, and common language.

two countries are less likely to vote in agreement with other countries. Considering that the majority of votes are “yes”, this implies among other things that USA and ISR are more likely to vote “no” than other countries. The posterior mean of the range parameter  $\kappa$  for the additive effects is a 4.001, indicating a relatively strong memory up to lag 3 or lag 4.



FIGURE 6. Posterior mean estimates for the additive random effect estimates  $\alpha^t$ .

Since the DAME model (2) depends on  $\mathbf{u}$  and  $\mathbf{D}$  only through  $\mathbf{u}'\mathbf{D}\mathbf{u}$ , to preserve identifiability we calculate an eigen-decomposition on every posterior matrix  $\mathbf{u}'\mathbf{D}\mathbf{u}$ , then take  $\mathbf{D}$  to be the diagonal matrix of eigenvalues and  $\mathbf{u}$  the corresponding matrix of eigenvectors. Figure 7 shows that most eigenvalues are positive, implying general tendency of positive homophily in the countries' latent positions.

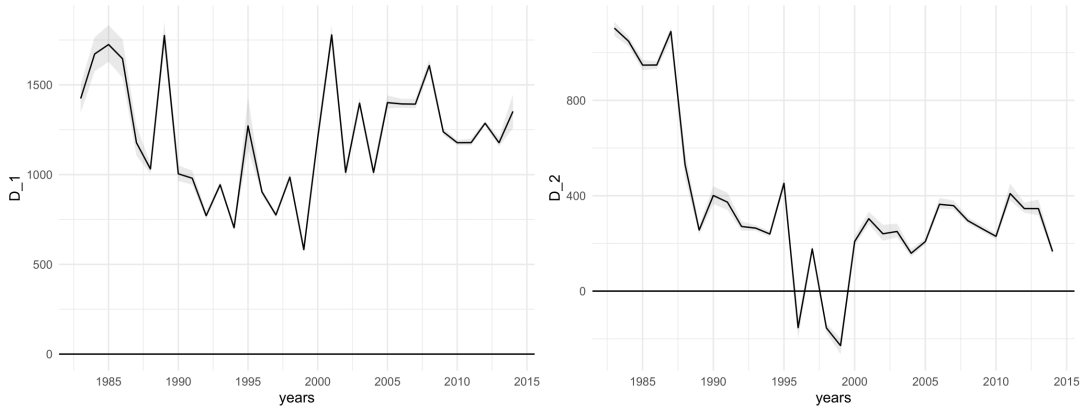


FIGURE 7. Posterior mean estimates and 95% credible intervals for the eigenvalues  $d_1^t$  and  $d_2^t$  from the eigen-decompositions of  $\mathbf{u}^{t'}\mathbf{D}^t\mathbf{u}^t$  in the 32 years from  $t = 1983$  to  $t = 2014$ .

In year 1996, 1998, and 1999, the eigenvalues in the second dimension ( $r=2$ ) are negative, implying the possible existence of anti-homophily. The posterior mean of the range parameter  $\kappa$  for the first and second dimension of  $\mathbf{u}$  is 10.874 and 0.867, indicating the first dimension of the latent position has a strong and long memory while the second dimension has a short memory similar to Markovian one.

To visualize the latent multiplicative-effect positions, we apply a Procrustes transformation of each  $\mathbf{u}^t\sqrt{\mathbf{D}^t}$  with  $\mathbf{u}^{t-1}\sqrt{\mathbf{D}^{t-1}}$  as the target matrix. In Figure 8, we plotted the scaled latent positions  $u_1^t\sqrt{d_1^t}$  vs  $u_2^t\sqrt{|d_2^t|}$ . When  $d_1^t > 0$  and  $d_2^t > 0$ , countries close together and far from the origin have higher propensity to agree in their UN voting patterns. When  $d_2^t < 0$ , such as year 1996 (as shown in Figure 8 with y-axis highlighted in red), countries close in their x-axis and far away in their y-axis have higher propensity to agree in their UN voting patterns.

We see interesting patterns of clustering of countries over time. Over the years, the most consistent pattern we observe from the latent space is a cluster of the USA and its close allies. For example, in 1984 – this is the later stage of the Cold War, US (USA, higher right hand side of the plot) is clustered with a number of countries, all of them are close US allies: United Kingdom (UKG), Israel (ISR), West Germany (GMY), Japan (JPN), France (FRN), and Australia (AUL). On the other side of the latent space locate mostly the non-US-ally countries such as Egypt (EGY), Iraq (IRQ), and Syria (SYR). Four years later, in 1988, this is a few years before the end of the Cold War, the 1984 pattern persisted; the US cluster we observed in 1988 almost stayed the same with the only exception being Australia (AUL) that moved to mid-way between the US cluster the rest of the countries in the latent space. However, in 1992, Australia (AUL) moved back to the US cluster which now also included Korea Republic (ROK) and Russia (RUS). Russia's location in this year reflects the Honeymoon period between the newly independent Russia and the United States right after the collapse of the Soviet Union. Indeed, after the end of the Cold War, diplomatic relations between the US and Russia improved until the end of the late 1990s. For example, both nations signed an arms control treaty in early 1993; they bilateral trade also increased.

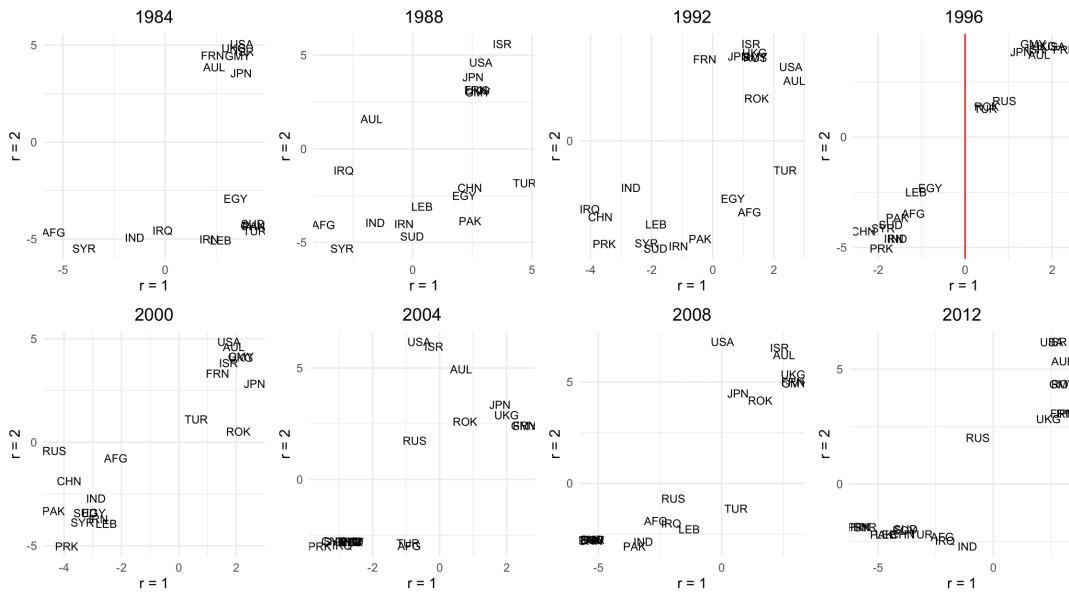


FIGURE 8. Posterior mean estimates of the multiplicative random effects  $u_i^t \sqrt{D^t}$  for 21 selected countries for every 4 years between  $t = 1984$  and  $t = 2012$ . For 1996, the solid line of the y-axis indicates a negative  $d_2$  value.

However, the US-Russia relations began to deteriorate in the late 1990s, starting in 1997 when NATO offered membership to Hungary, Poland, and the Czech Republic. Russia's position in the latent space reflects such a change in relationship. For example, in 2000, Russia (RUS) has moved to the opposite side from the US cluster. In all later years shown in the plots, 2004, 2008, and 2012, Russia never rejoined the US cluster, which reflects the tensions between the two countries ever since the NATO expansion in the late 1990s. We see that in 1992 and 2000, countries lie in two clusters and they vote in great agreement within their cluster. This implies high transitivity. On the other hand, in 1996, countries' voting behaviors are similar within a cluster but their votes do not necessarily agree with those within their cluster. This demonstrates stochastic equivalence. Our model captures both of these network features through the multiplicative effects  $u$  and the sign of  $D$ .

**5. Discussion.** As an extension of the additive and multiplicative effects (AME) model, the dynamic additive and multiplicative effects (DAME) network model can flexibly learn the underlying time-varying structure in dynamic networks, while inferring the effects of node-specific and dyad-specific latent variables. Accounting for the correlation structure of the networks makes better use of dynamic networks than modeling them as separate network snapshots. The visualization of the model-estimated time-varying parameters provides an effective temporal trend analysis of dynamic networks, as well as the descriptive visualization of higher-order dependence over time. In modeling UN voting behavior, the example that has motivated our model, we find that having alliances, active trade, and common languages are positively associated with countries' voting similarities. The nodal effects indicate that USA and Israel are generally less likely to vote in agreement with other countries. After controlling for the known factors in the studies of international relations and nodal heterogeneity, the multiplicative effects reveal interesting clustering patterns in the latent space, such as the allies of USA, and their position changes relative to the Soviet Union and Russia, before and after the Cold War. These particular data display both positive and negative homophily over time which showcase the advantage of the model, however, the methodology proposed here goes beyond this particular example and can be applied to a wide range of applications.

Several extensions and modifications of this work are possible. If researchers are interested in the determining factors in changes of voting behaviors, we could include  $Y_{t-1}$  in the model, as in [Friel et al. \(2016\)](#). Given the evidence found in the data that the current year’s outcome highly depends on the previous year, this additional term could also improve the goodness of fit of the model. In addition, our model assumes a common variance for all additive effects. With the added time dimension, more complicated models with heterogeneous additive effects are possible.

Although we illustrate the entire framework in the context of symmetric or undirected networks, it is straightforward to apply the same dynamic extension to the directed version of the additive and multiplicative effects model of [Hoff \(2021\)](#). Furthermore, our framework can be applied to binary and ordinal network data with appropriate link functions.

We have avoided any sort of formal model-selection criterion in choosing the value of  $R$ , the dimension of the latent multiplicative effect space. For the UNGA voting data, we settled on  $R = 2$  based on informal exploration suggesting that increasing the dimension does not markedly improve the model fit. For instance, the estimated posterior eigenvalue  $d_3^t$  was roughly zero for all  $t = 1, \dots, T$ . There exists the possibility of developing a more rigorous method of selecting this dimension.

Finally, considering the increasing ubiquity of large network datasets with time granularity, future work might focus on improving the computational efficiency of the fitting algorithm. Our current MCMC algorithm mixes slowly, taking over 72 hours to achieve full convergence of all fixed and random effects for the UNGA dataset. Surely this performance could be improved.

## SUPPLEMENTARY MATERIAL

### **A. Derivations of Full Conditional Distributions**

This section provides the derivations of the full conditional distributions for estimating the model parameters.

### **B. Metropolis-Hastings Algorithm for GP Parameters**

This section describes the Metropolis-Hastings Algorithms for estimating the Gaussian Process parameters in the model.

### **C. List of Countries in Voting Network**

This section provides the full list of countries in the UN voting network.

### **D. Summary Statistics**

This section presents exploratory data analysis statistics of the dynamic voting data, including summary statistics of the total votes and important votes, and associations among the predictors used in the model.

### **E. Posterior Predictive Statistics for the United States (USA)**

This section presents boxplots of posterior predictive degree statistics of four models U.S.A.

### **F. Residual Diagnostics**

This section presents the residual plots and additional simulations to demonstrate the robustness of the model to mis-specification of the error distribution.

### **G. Posterior Summaries on GP Parameters**

This section presents tables that describe the posterior distributions of the Gaussian Process parameters.

### **H. Posterior Predictive Checks**

This section presents posterior predictive plots of the overall degree distributions aggregating all nodes and time points.

## REFERENCES

- Bailey, M. A., A. Strezhnev, and E. Voeten (2017). Estimating dynamic state preferences from United Nations voting data. *Journal of Conflict Resolution* 61(2), 430–456.
- Durante, D. and D. B. Dunson (2014). Nonparametric Bayes dynamic modelling of relational data. *Biometrika* 101(4), 883–898.
- Friel, N., R. Rastelli, J. Wyse, and A. E. Raftery (2016). Interlocking directorates in Irish companies using a latent space model for bipartite networks. *Proceedings of the National Academy of Sciences* 113(24), 6629–6634.
- Gartzke, E. (1998). Kant we all just get along? Opportunity, willingness, and the origins of the democratic peace. *American Journal of Political Science* 42, 1–27.
- Gartzke, E. (2000). Preferences and the democratic peace. *International Studies Quarterly* 44(2), 191–212.
- Gelman, A. (2006). Prior distributions for variance parameters in hierarchical models (comment on article by browne and draper). *Bayesian Analysis* 1(3), 515–534.
- Gibler, D. M. (2008). *International military alliances, 1648-2008*. CQ Press.
- Goodreau, S. M., J. A. Kitts, and M. Morris (2009). Birds of a feather, or friend of a friend? using exponential random graph models to investigate adolescent social networks. *Demography* 46(1), 103–125.
- Hanneke, S., W. Fu, E. P. Xing, et al. (2010). Discrete temporal models of social networks. *Electronic Journal of Statistics* 4, 585–605.
- Hoff, P. (2021). Additive and multiplicative effects network models. *Statistical Science* 36(1), 34–50.
- Hoff, P. D. (2005). Bilinear mixed-effects models for dyadic data. *Journal of the American Statistical Association* 100(469), 286–295.
- Hoff, P. D., A. E. Raftery, and M. S. Handcock (2002). Latent space approaches to social network analysis. *Journal of the American Statistical Association* 97(460), 1090–1098.
- Hunter, D. R., S. M. Goodreau, and M. S. Handcock (2008). Goodness of fit of social network models. *Journal of the American Statistical Association* 103(481), 248–258.
- Kim, B., K. H. Lee, L. Xue, X. Niu, et al. (2018). A review of dynamic network models with latent variables. *Statistics Surveys* 12, 105–135.
- Kim, B., X. Niu, D. Hunter, and X. Cao (2023). Supplement to “a dynamic additive and multiplicative effects network model with application to the united nations voting behaviors”.
- Krivitsky, P. N. and M. S. Handcock (2014). A separable model for dynamic networks. *Journal of the Royal Statistical Society. Series B, Statistical Methodology* 76(1), 29–46.
- Leibenstein, H. (1966). Shaping the world economy: Suggestions for an international economic policy.
- Lusher, D., J. Koskinen, and G. Robins (2013). *Exponential random graph models for social networks: Theory, methods, and applications*. Cambridge University Press.
- Marshall, M. G., K. Jagers, and T. R. Gurr (2014). Polity IV annual time-series, 1800–2013. *Center for International Development and Conflict Management at the University of Maryland College Park*.
- Olivella, S., T. Pratt, and K. Imai (2022). Dynamic stochastic blockmodel regression for network data: Application to international militarized conflicts. *Journal of the American Statistical Association*.
- Rasmussen, C. E. (2003). Gaussian processes in machine learning. In *Summer School on Machine Learning*, pp. 63–71. Springer.
- Rodrigue, J.-P., C. Comtois, and B. Slack (2016). *The geography of transport systems*. Routledge.
- Sewell, D. K. and Y. Chen (2015). Latent space models for dynamic networks. *Journal of the American Statistical Association* 110(512), 1646–1657.
- Signorino, C. S. and J. M. Ritter (1999). Tau-b or not tau-b: Measuring the similarity of foreign policy positions. *International Studies Quarterly* 43(1), 115–144.
- Snijders, T. A., G. G. Van de Bunt, and C. E. Steglich (2010). Introduction to stochastic actor-based models for network dynamics. *Social Networks* 32(1), 44–60.
- Snijders, T. A. B. (2001). The statistical evaluation of social network dynamics. *Sociological Methodology* 31(1), 361–395.
- Voeten, E. (2013). Data and analyses of voting in the UN general assembly. In B. Reinalda (Ed.), *Routledge Handbook of International Organization*. Routledge. Available at SSRN: <http://ssrn.com/abstract=2111149>.
- Ward, M. D. and P. D. Hoff (2007). Persistent patterns of international commerce. *Journal of Peace Research* 44(2), 157–175.
- Zellner, A. (1986). On assessing prior distributions and bayesian regression analysis with g-prior distributions. In P. K. Goel and A. Zellner (Eds.), *Bayesian inference and decision techniques: Essays in Honor of Bruno de Finetti (Studies in Bayesian Econometrics and Statistics, Vol 6)*, pp. 233–243. Amsterdam: North-Holland.

# Supplementary Materials to: “A Dynamic Additive and Multiplicative Effects Network Model with Application to the United Nations Voting Behaviors ”

## A Derivations of Full Conditional Distributions

The noise error variance  $\sigma_e^2$  has a conditional inverse-gamma distribution with parameters as derived below:

$$\begin{aligned}
 & \Pr(\sigma_e^2 | \mathbf{Y}, k_\sigma, \theta_\sigma) \propto \Pr(\mathbf{Y} | \mathbf{X}, \boldsymbol{\beta}, \mathbf{a}, \mathbf{d}, \mathbf{u}, \sigma_e^2) \times \Pr(\sigma_e^2 | k_\sigma, \theta_\sigma) \\
 & \propto \prod_{t=1}^T \prod_{i>j} (\sigma_e^2)^{-\frac{1}{2}} \exp \left\{ -\frac{1}{2\sigma_e^2} \left\| y_{ij}^t - \left( \sum_{p=1}^P \beta_p^t X_{ijp}^t + a_i^t + a_j^t + \mathbf{u}_i^{t'} \mathbf{D}^t \mathbf{u}_j^t \right) \right\|^2 \right\} \times (\sigma_e^2)^{-k_\sigma - 1} \exp \left\{ \frac{1}{\sigma_e^2} \theta_\sigma \right\} \\
 & = (\sigma_e^2)^{-\frac{T \cdot N(N-1)}{2} - k_\sigma - 1} \times \exp \left\{ -\frac{1}{\sigma_e^2} \left( \frac{1}{2} \sum_{t=1}^T \sum_{i>j} \left\| y_{ij}^t - \left( \sum_{p=1}^P \beta_p^t X_{ijp}^t + a_i^t + a_j^t + \mathbf{u}_i^{t'} \mathbf{D}^t \mathbf{u}_j^t \right) \right\|^2 + \theta_\sigma \right) \right\} \\
 & \sim \mathcal{IG} \left( \frac{T \cdot N(N-1)}{4} + k_\sigma, \quad \frac{1}{2} \sum_{t=1}^T \sum_{i>j} (E_{ij}^t)^2 + \theta_\sigma \right)
 \end{aligned}$$

The fixed-effect coefficient  $\boldsymbol{\beta}_p$ , for  $1 \leq p \leq P$ , has a conditional multivariate normal distribution with parameters as derived below:

$$\begin{aligned}
& \Pr(\boldsymbol{\beta}_p | \mathbf{Y}, \mathbf{X}, \kappa_p^\beta, \tau_p^\beta) \propto \Pr(\mathbf{Y} | \mathbf{X}, \boldsymbol{\beta}_p, \boldsymbol{\beta}_{[-p]}, \mathbf{a}, \mathbf{d}, \mathbf{u}, \sigma_e^2) \times \Pr(\boldsymbol{\beta}_p | \kappa_p^\beta, \tau_p^\beta) \\
& \propto \prod_{i>j} \exp\left\{-\frac{1}{2\sigma_e^2} \|\mathbf{E}_{ij[-p]} - \mathbf{X}_{ijp}\boldsymbol{\beta}_p\|^2\right\} \times \exp\left\{-\frac{1}{2}(\boldsymbol{\beta}_p'(\Sigma_p^\beta)^{-1}\boldsymbol{\beta}_p)\right\} \\
& \quad \text{where } \mathbf{E}_{ij[-p]} = \{E_{ij[-p]}^t\}_{t=1}^T \text{ (with } E_{ij[-p]}^t = E_{ij}^t + \beta_p^t X_{ijp}^t) \text{ and } \mathbf{X}_{ijp} = \{X_{ijp}^t\}_{t=1}^T \\
& \propto \exp\left\{-\frac{1}{2\sigma_e^2} \left(\sum_{i>j} -2(\mathbf{E}_{ij[-p]}\mathbf{X}_{ijp})'\boldsymbol{\beta}_p + \boldsymbol{\beta}_p'(\text{diag}(\sum_{i>j} \mathbf{X}_{ijp}^2))\boldsymbol{\beta}_p)\right)\right\} \times \exp\left\{-\frac{1}{2}(\boldsymbol{\beta}_p'(\Sigma_p^\beta)^{-1}\boldsymbol{\beta}_p)\right\} \\
& \propto \exp\left\{-\frac{1}{2}(\boldsymbol{\beta}_p'((\Sigma_p^\beta)^{-1} + \frac{\text{diag}(\sum_{i>j} \mathbf{X}_{ijp}^2)}{\sigma_e^2})\boldsymbol{\beta}_p - \frac{2}{\sigma_e^2}(\sum_{i>j}(\mathbf{E}_{ij[-p]}\mathbf{X}_{ijp})'\boldsymbol{\beta}_p))\right\} \\
& \sim \mathcal{N}_T(\tilde{\boldsymbol{\mu}}_{\beta_p}, \tilde{\Sigma}_{\beta_p}), \\
& \quad \text{where } \tilde{\Sigma}_{\beta_p} = \left[(\Sigma_p^\beta)^{-1} + \frac{\text{diag}(\{\sum_{i>j} X_{ijp}^2\}_{t=1}^T)}{\sigma_e^2}\right]^{-1} \text{ and } \tilde{\boldsymbol{\mu}}_{\beta_p} = \left[\frac{\{\sum_{i>j}(E_{ij[-p]}^t X_{ijp}^t)\}_{t=1}^T}{\sigma_e^2}\right] \tilde{\Sigma}_{\beta_p}.
\end{aligned}$$

The  $T$ -dimensional additive random effect  $\mathbf{a}_i$ , for  $1 \leq i \leq N$ , has a conditional multivariate normal distribution with parameters as derived below:

$$\begin{aligned}
& \Pr(\mathbf{a}_i | \mathbf{Y}, \kappa^a, \tau^a) \propto \prod_{j \neq i} \Pr(\mathbf{Y} | \mathbf{X}, \boldsymbol{\beta}, \mathbf{a}_i, \mathbf{a}_{[-i]}, \mathbf{d}, \mathbf{u}, \sigma_e^2) \times \Pr(\mathbf{a}_i | \kappa^a, \tau^a) \\
& \propto \prod_{j \neq i} \exp\left\{-\frac{1}{2\sigma_e^2} \|\mathbf{E}_{ij[-i]} - \mathbf{a}_i\|^2\right\} \times \exp\left\{-\frac{1}{2}(\mathbf{a}_i'(\Sigma^a)^{-1}\mathbf{a}_i)\right\} \\
& \quad \text{where } \mathbf{E}_{ij[-i]} = \{E_{ij[-i]}^t\}_{t=1}^T \text{ with } E_{ij[-i]}^t = E_{ij}^t + \mathbf{a}_i^t \\
& \propto \exp\left\{-\frac{1}{2\sigma_e^2} \left(\sum_{j \neq i} -2(\mathbf{E}_{ij[-i]})'\mathbf{a}_i + \mathbf{a}_i'(\sum_{j \neq i} I_T)\mathbf{a}_i\right)\right\} \times \exp\left\{-\frac{1}{2}(\mathbf{a}_i'(\Sigma^a)^{-1}\mathbf{a}_i)\right\} \\
& \propto \exp\left\{-\frac{1}{2}(\mathbf{a}_i'((\Sigma^a)^{-1} + \frac{(N-1)I_T}{\sigma_e^2})\mathbf{a}_i - \frac{2}{\sigma_e^2}(\sum_{j \neq i}(\mathbf{E}_{ij[-i]})'\mathbf{a}_i))\right\} \\
& \sim \mathcal{N}_T(\tilde{\boldsymbol{\mu}}_{a_i}, \tilde{\Sigma}_{a_i}), \\
& \quad \text{where } \tilde{\Sigma}_{a_i} = \left[(\Sigma^a)^{-1} + \frac{(N-1)I_T}{\sigma_e^2}\right]^{-1} \text{ and } \tilde{\boldsymbol{\mu}}_{a_i} = \left[\frac{\{\sum_{j \neq i} E_{ij[-i]}^t\}_{t=1}^T}{\sigma_e^2}\right] \tilde{\Sigma}_{a_i}.
\end{aligned}$$

The  $T$ -dimensional latent vector of the multiplicative random effect  $\mathbf{u}_{ir}$ , for  $1 \leq i \leq N$  and  $1 \leq r \leq R$ , has a conditional multivariate normal distribution with parameters as derived below:

$$\begin{aligned}
& \Pr(\mathbf{u}_{ir} | \mathbf{Y}, \kappa_r^u, \tau_r^u) \propto \Pr(\mathbf{Y} | \mathbf{X}, \boldsymbol{\beta}, \mathbf{a}, \mathbf{d}, \mathbf{u}_{ir}, \mathbf{u}_{[-ir]}, \sigma_e^2) \times \Pr(\mathbf{u}_{ir} | \kappa_r^u, \tau_r^u) \\
& \propto \prod_{i=1}^N \prod_{j \neq i} \exp \left\{ -\frac{1}{2\sigma_e^2} \|\mathbf{E}_{ij[-r]} - \mathbf{u}'_{ir} \mathbf{d}_r \mathbf{u}_{jr}\|^2 \right\} \times \exp \left\{ -\frac{1}{2} (\mathbf{u}'_{ir} (\Sigma_r^u)^{-1} \mathbf{u}_{ir}) \right\} \\
& \quad \text{where } \mathbf{E}_{ij[-r]} = \{E_{ij[-r]}^t\}_{t=1}^T \text{ (with } E_{ij[-r]}^t = E_{ij}^t + u_{ir}^t d_r^t u_{jr}^t \text{)} \text{ and } \mathbf{u}'_{ir} \mathbf{d}_r \mathbf{u}_{jr} = \{u_{ir}^t d_r^t u_{jr}^t\}_{t=1}^T \\
& \propto \exp \left\{ -\frac{1}{4\sigma_e^2} \left( \sum_{j \neq i} -2(\mathbf{E}_{ij[-r]} \mathbf{d}_r \mathbf{u}_{jr})' \mathbf{u}_{ir} + \mathbf{u}'_{ir} (\text{diag}(\mathbf{d}_r^2 \sum_{j \neq i} \mathbf{u}_{jr}^2)) \mathbf{u}_{ir} \right) \right\} \times \exp \left\{ -\frac{1}{2} (\mathbf{u}'_{ir} (\Sigma_r^u)^{-1} \mathbf{u}_{ir}) \right\} \\
& \propto \exp \left\{ -\frac{1}{2} \left( \mathbf{u}'_{ir} ((\Sigma_r^u)^{-1} + \frac{1}{2} \times \frac{\text{diag}(\mathbf{d}_r^2 \sum_{j \neq i} \mathbf{u}_{jr}^2)}{\sigma_e^2}) \mathbf{u}_{ir} - \frac{2}{\sigma_e^2} \left( \frac{1}{2} \sum_{j \neq i} (\mathbf{E}_{ij[-r]} \mathbf{d}_r \mathbf{u}_{jr})' \mathbf{u}_{ir} \right) \right) \right\} \\
& \sim \mathcal{N}_T(\tilde{\mu}_{u_{ir}}, \tilde{\Sigma}_{u_{ir}}), \\
& \text{where } \tilde{\Sigma}_{u_{ir}} = \left[ (\Sigma_r^u)^{-1} + \frac{\text{diag}(\{(d_r^t)^2 \sum_{j \neq i} (u_{jr}^t)^2\}_{t=1}^T)}{2\sigma_e^2} \right]^{-1} \text{ and } \tilde{\mu}_{u_{ir}} = \left[ \frac{\{\sum_{j \neq i} (E_{ij[-r]}^t d_r^t u_{jr}^t)\}_{t=1}^T}{2\sigma_e^2} \right] \tilde{\Sigma}_{u_{ir}}.
\end{aligned}$$

The  $T$ -dimensional vector of the  $r$ th eigenvalue of the multiplicative random effect  $\mathbf{d}_r$ , for  $1 \leq r \leq R$ , has a conditional multivariate normal distribution with parameters as derived below:

$$\begin{aligned}
& \Pr(\mathbf{d}_r | \mathbf{Y}) \propto \Pr(\mathbf{Y} | \mathbf{X}, \boldsymbol{\beta}, \mathbf{a}, \mathbf{d}_r, \mathbf{d}_{[-r]}, \mathbf{u}, \sigma_e^2) \times \Pr(\mathbf{d}_r) \\
& \propto \prod_{i>j} \exp \left\{ -\frac{1}{2\sigma_e^2} \|\mathbf{E}_{ij[-r]} - \mathbf{u}'_{ir} \mathbf{d}_r \mathbf{u}_{jr}\|^2 \right\} \times \exp \left\{ -\frac{1}{2} (\mathbf{d}'_r \mathbf{d}_r) \right\} \\
& \quad \text{where } \mathbf{E}_{ij[-r]} = \{E_{ij[-r]}^t\}_{t=1}^T \text{ (with } E_{ij[-r]}^t = E_{ij}^t + u_{ir}^t d_r^t u_{jr}^t \text{)} \text{ and } \mathbf{u}'_{ir} \mathbf{d}_r \mathbf{u}_{jr} = \{u_{ir}^t d_r^t u_{jr}^t\}_{t=1}^T \\
& \propto \exp \left\{ -\frac{1}{2\sigma_e^2} \left( \sum_{i>j} -2(\mathbf{E}_{ij[-r]} \mathbf{u}_{ir} \mathbf{u}_{jr})' \mathbf{d}_r + \mathbf{d}'_r (\text{diag}(\sum_{i>j} (\mathbf{u}_{ir} \mathbf{u}_{jr})^2)) \mathbf{d}_r \right) \right\} \times \exp \left\{ -\frac{1}{2} (\mathbf{d}'_r \mathbf{d}_r) \right\} \\
& \propto \exp \left\{ -\frac{1}{2} \left( \mathbf{d}'_r (I_T + \frac{\text{diag}(\sum_{i>j} (\mathbf{u}_{ir} \mathbf{u}_{jr})^2)}{\sigma_e^2}) \mathbf{d}_r - \frac{2}{\sigma_e^2} \left( \sum_{i>j} (\mathbf{E}_{ij[-r]} \mathbf{u}_{ir} \mathbf{u}_{jr})' \mathbf{d}_r \right) \right) \right\} \\
& \sim \mathcal{N}_T(\tilde{\mu}_{d_r}, \tilde{\Sigma}_{d_r}), \\
& \text{where } \tilde{\Sigma}_{d_r} = \left[ I_T + \frac{\text{diag}(\{\sum_{i>j} (u_{ir}^t u_{jr}^t)^2\}_{t=1}^T)}{\sigma_e^2} \right]^{-1} \text{ and } \tilde{\mu}_{d_r} = \left[ \frac{\{\sum_{i>j} (E_{ij[-r]}^t u_{ir}^t u_{jr}^t)\}_{t=1}^T}{\sigma_e^2} \right] \tilde{\Sigma}_{d_r}.
\end{aligned}$$

## B Metropolis-Hastings Algorithm for GP Parameters

For the Gaussian process variance parameter  $\tau$  and length-scale parameter  $\kappa$ , we use the Metropolis-Hastings algorithm with a proposal density  $Q$  being the multivariate Gaussian distribution with a diagonal covariance matrix—i.e.,  $\text{diag}(\sigma_{Q1}^2, \sigma_{Q2}^2)$ . Given the proposal variance  $\sigma_Q^2 = (\sigma_{Q1}^2, \sigma_{Q2}^2)$ , we sample the new values  $\tau'$  and  $\kappa'$  from

$$(p', q') \sim \mathcal{N}_2((p, q), \text{diag}(\sigma_Q^2)),$$

where  $p = \log(\tau)$  and  $q = \log(\kappa)$ . We use change of variables and sample from a bivariate normal with mean  $(p, q) = \log(\tau, \kappa)$  since both  $\tau$  and  $\kappa$  have to be positive. Under the symmetric proposal distribution as above, we accept the new proposed value  $(\tau', \kappa') = (\exp(p'), \exp(q'))$  with probability equal to

$$\min \left\{ 1, \frac{\Pr(p'', q'' | \boldsymbol{\eta}, k_\eta, \theta_\eta, \gamma)}{\Pr(p^n, q^n | \boldsymbol{\eta}, k_\eta, \theta_\eta, \gamma)} \right\},$$

where  $\boldsymbol{\eta} = (\eta_1, \dots, \eta_T)$  can be any of  $\boldsymbol{\beta}$ ,  $\mathbf{a}$ , or  $\mathbf{u}$ , depending on the situation. After taking account of the Jacobian,  $\Pr_{p,q}(p'', q'' | \boldsymbol{\eta}, k_\eta, \theta_\eta, \gamma) = \Pr_{\tau,\kappa}((\exp(p''), (\exp(q'')) | \boldsymbol{\eta}, k_\eta, \theta_\eta, \gamma) \times \exp(p'') \times \exp(q'')$ .

Below are the acceptance ratios for all pairs of variables. In each case,  $\tau$  has an  $\mathcal{IG}(k_\eta, \theta_\eta)$  prior and  $\kappa$  has an independent half-Cauchy( $\gamma_\eta$ ) prior.

1.  $(\tau_p^\beta, \kappa_p^\beta)$ , for  $p = 1, \dots, P$ :

$$\begin{aligned} \frac{\Pr(\tau_p^{\beta'}, \kappa_p^{\beta'} | \boldsymbol{\beta}_p, k_\beta, \theta_\beta, \gamma_\beta) \times \tau_p^{\beta'} \kappa_p^{\beta'}}{\Pr(\tau_p^\beta, \kappa_p^\beta | \boldsymbol{\beta}_p, k_\beta, \theta_\beta, \gamma_\beta) \times \tau_p^\beta \kappa_p^\beta} &= \frac{\Pr(\tau_p^{\beta'}, \kappa_p^{\beta'}, \boldsymbol{\beta}_p | k_\beta, \theta_\beta, \gamma_\beta) \times \tau_p^{\beta'} \kappa_p^{\beta'}}{\Pr(\tau_p^\beta, \kappa_p^\beta, \boldsymbol{\beta}_p | k_\beta, \theta_\beta, \gamma_\beta) \times \tau_p^\beta \kappa_p^\beta} \\ &= \frac{\Pr(\tau_p^{\beta'} | k_\beta, \theta_\beta) \Pr(\kappa_p^{\beta'} | \gamma_\beta) \Pr(\boldsymbol{\beta}_p | \tau_p^{\beta'}, \kappa_p^{\beta'}) \times \tau_p^{\beta'} \kappa_p^{\beta'}}{\Pr(\tau_p^\beta | k_\beta, \theta_\beta) \Pr(\kappa_p^\beta | \gamma_\beta) \Pr(\boldsymbol{\beta}_p | \tau_p^\beta, \kappa_p^\beta) \times \tau_p^\beta \kappa_p^\beta}, \end{aligned}$$

where  $\boldsymbol{\beta}_p \sim \mathcal{N}_T(\mathbf{0}, \Sigma_p^\beta)$  with  $\Sigma_p^\beta = \tau_p^\beta f(\kappa_p^\beta)$ .

2.  $(\tau^a, \kappa^a)$

$$\begin{aligned} \frac{\Pr(\tau^{a'}, \kappa^{a'} | \mathbf{a}, k_a, \theta_a, \gamma_a) \times \tau^{a'} \kappa^{a'}}{\Pr(\tau^a, \kappa^a | \mathbf{a}, k_a, \theta_a, \gamma_a) \times \tau^a \kappa^a} &= \frac{\Pr(\tau^{a'}, \kappa^{a'}, \mathbf{a} | k_a, \theta_a, \gamma_a) \times \tau^{a'} \kappa^{a'}}{\Pr(\tau^a, \kappa^a, \mathbf{a} | k_a, \theta_a, \gamma_a) \times \tau^a \kappa^a} \\ &= \frac{\Pr(\tau^{a'} | k_a, \theta_a) \Pr(\kappa^{a'} | \gamma_a) \prod_{i=1}^N \Pr(\mathbf{a}_i | \tau^{a'}, \kappa^{a'}) \times \tau^{a'} \kappa^{a'}}{\Pr(\tau^a | k_a, \theta_a) \Pr(\kappa^a | \gamma_a) \prod_{i=1}^N \Pr(\mathbf{a}_i | \tau^a, \kappa^a) \times \tau^a \kappa^a}, \end{aligned}$$

where  $\mathbf{a}_i \sim \mathcal{N}_T(\mathbf{0}, \Sigma^a)$  with  $\Sigma^a = \tau^a f(\kappa^a)$ .

3.  $(\tau_r^u, \kappa_r^u)$ , for  $r = 1, \dots, R$ :

$$\begin{aligned} \frac{\Pr(\tau_r^{u'}, \kappa_r^{u'} | \mathbf{u}_r, k_u, \theta_u, \gamma_u) \times \tau_r^{u'} \kappa_r^{u'}}{\Pr(\tau_r^u, \kappa_r^u | \mathbf{u}_r, k_u, \theta_u, \gamma_u) \times \tau_r^u \kappa_r^u} &= \frac{\Pr(\tau_r^{u'}, \kappa_r^{u'}, \mathbf{u}_r | k_u, \theta_u, \gamma_u) \times \tau_r^{u'} \kappa_r^{u'}}{\Pr(\tau_r^u, \kappa_r^u, \mathbf{u}_r | k_u, \theta_u, \gamma_u) \times \tau_r^u \kappa_r^u} \\ &= \frac{\Pr(\tau_r^{u'} | k_u, \theta_u) \Pr(\kappa_r^{u'} | \gamma_u) \prod_{i=1}^N \Pr(\mathbf{u}_{ir} | \tau_r^{u'}, \kappa_r^{u'}) \times \tau_r^{u'} \kappa_r^{u'}}{\Pr(\tau_r^u | k_u, \theta_u) \Pr(\kappa_r^u | \gamma_u) \prod_{i=1}^N \Pr(\mathbf{u}_{ir} | \tau_r^u, \kappa_r^u) \times \tau_r^u \kappa_r^u}, \end{aligned}$$

where  $\mathbf{u}_{ir} \sim \mathcal{N}_T(\mathbf{0}, \Sigma_r^u)$  with  $\Sigma_r^u = \tau_r^u f(\kappa_r^u)$ .

## C List of Countries in Voting Network

Abbreviation	Country or area name	Abbreviation	Country or area name
AFG*	Afghanistan	KUW	Kuwait
ALB	Albania	LEB*	Lebanon
ALG	Algeria	LIB	Libya
ANG	Angola	MAA	Mauritania
ARG	Argentina	MEX	Mexico
AUL*	Australia	MLI	Mali
BAH	Bahrain	MOR	Morocco
BEN	Benin	MZM	Mozambique
BFO	Burkina Faso	NEW	New Zealand
BNG	Bangladesh	NIC	Nicaragua
BOL	Bolivia	NIG	Nigeria
BRA	Brazil	NIR	Niger
BUI	Burundi	NOR	Norway
BUL	Bulgaria	NTH	Netherlands
CAN	Canada	OMA	Oman
CAO	Cameroon	PAK*	Pakistan
CEN	Central African Republic	PAN	Panama
CHL	Chile	PAR	Paraguay
CHN*	China	PER	Peru
COL	Colombia	PHI	Philippines
CON	Congo	POL	Poland
COS	Costa Rica	POR	Portugal
DEN	Denmark	PRK*	North Korea
DOM	Dominican Republic	QAT	Qatar
ECU	Ecuador	ROK*	South Korea
EGY*	Egypt	RUS*	Russia
FIN	Finland	RWA	Rwanda
FRN*	France	SAL	El Salvador
GAB	Gabon	SAU	Saudi Arabia
GAM	Gambia	SEN	Senegal
GMY*	Germany	SIE	Sierra Leone
GHA	Ghana	SPN	Spain
GRC	Greece	SUD*	Sudan
GUA	Guatemala	SUR	Suriname
GUI	Guinea	SYR*	Syrian Arab Republic
GUY	Guyana	TAZ	Tanzania
HAI	Haiti	TOG	Togo
HON	Honduras	TRI	Trinidad and Tobago
HUN	Hungary	TUN	Tunisia
IND*	India	TUR*	Turkey
INS	Indonesia	UAE	United Arab Emirates
IRN*	Iran (Islamic Republic of)	UGA	Uganda
IRQ*	Iraq	UKG*	United Kingdom
ISR*	Israel	URU	Uruguay
ITA	Italy	USA*	United States of America
JAM	Jambia	VEN	Venezuela
JOR	Jordan	ZAM	Zambia
JPN*	Japan	ZIM	Zimbabwe
KEN	Kenya		

Table 1: Full list of the 97 countries, where the 21 most active countries during the ten year period 2004–2014 according to ? are marked with \*.

## D Summary Statistics

Year	1983	1984	1985	1986	1987	1988	1989	1990	1991
Joint votes	126.709	128.302	134.563	139.387	133.998	123.612	104.472	78.943	61.753
Agreement	84.7	85.2	84.3	85.4	87.7	87.2	88.5	87.8	86.4
Year	1992	1993	1994	1995	1996	1997	1998	1999	2000
Joint votes	58.263	52.001	56.187	62.019	61.477	58.104	50.969	55.071	52.731
Agreement	84.2	83.5	84.7	83.5	84.4	83.1	85.1	83.7	83.9
Year	2001	2002	2003	2004	2005	2006	2007	2008	2009
Joint votes	50.362	58.282	63.418	61.860	59.651	73.235	64.857	62.353	57.893
Agreement	81.5	82.3	83.0	81.4	83.5	83.1	81.9	82.9	80.4
Year	2010	2011	2012	2013	2014				
Joint votes	57.336	54.404	60.216	56.016	66.197				
Agreement	82.2	79.8	82.3	80.2	81.4				

Table 2: Summary of the United Nations voting data for non-important votes: Average number of common votes (*upper*) and average voting similarity index (*lower*) per year.

Year	1983	1984	1985	1986	1987	1988	1989	1990	1991
Joint votes	7.384	7.441	8.129	9.201	8.283	5.121	12.605	7.361	8.559
Agreement	69.6	72.4	72.5	74.8	72.5	77.3	79.8	83.2	83.6
Year	1992	1993	1994	1995	1996	1997	1998	1999	2000
Joint votes	13.458	11.013	13.447	24.932	9.655	10.026	8.427	10.776	8.970
Agreement	80.6	77.3	78.5	82.7	76.5	80.5	77.6	82.9	76.8
Year	2001	2002	2003	2004	2005	2006	2007	2008	2009
Joint votes	9.191	12.826	12.142	8.432	8.855	10.956	10.681	10.845	10.946
Agreement	72.9	81.6	75.5	83.5	78.3	73.3	73.9	70.0	75.0
Year	2010	2011	2012	2013	2014				
Joint votes	12.289	9.067	7.575	10.171	12.048				
Agreement	74.4	75.1	73.3	75.4	84.7				

Table 3: Summary of the United Nations voting data for important votes: Average number of common votes (*upper*) and average voting similarity index (*lower*) per year.

correlation	log(distance)	polity	alliance	Trade/GDP	language
log(distance)	1.000	0.136	-0.508	-0.355	-0.286
polity	0.136	1.000	-0.264	-0.095	-0.142
alliance	-0.508	-0.264	1.000	0.275	0.417
Trade/GDP	-0.355	-0.095	0.275	1.000	0.100
language	-0.286	-0.142	0.417	0.100	1.000

Table 4: Pearson correlation coefficients between the observed dyadic covariates. Each variable is a  $\binom{97}{2} \times 32$ -dimensional vector resulting from vectorizing across all years and all off-diagonal entries of the covariate matrices. Two of the covariates, log(distance) and language, do not vary over time.

## E Posterior Predictive Statistics for the United States (USA)

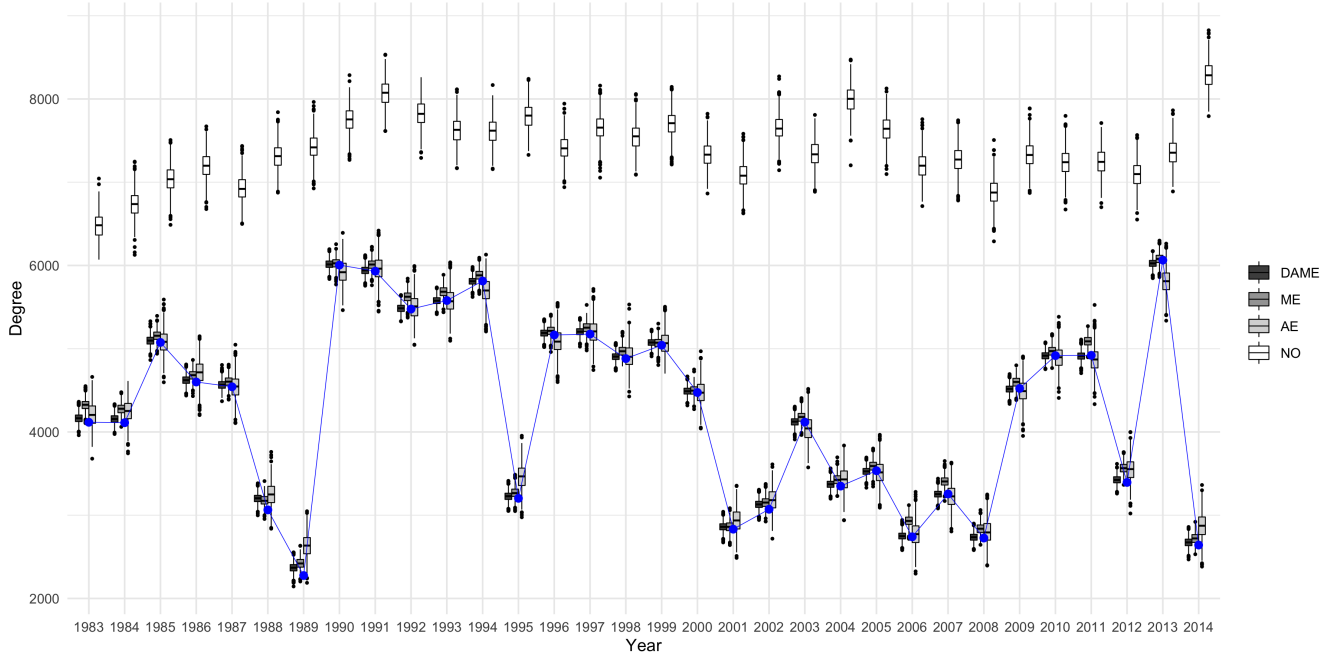


Figure 1: Boxplots of 1,000 posterior predictive degree statistics for the United States (USA) for four models: The full DAME with both additive and multiplicative effects, the multiplicative effects only model ME, the additive effects only model AE, and the model NO with neither. The dots show the observed statistics.

## F Residual Diagnostics

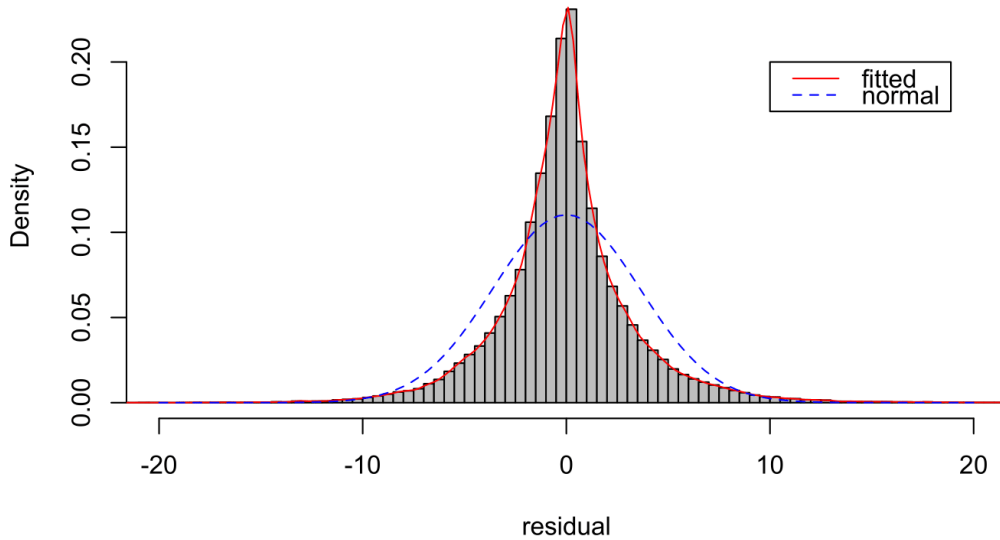


Figure 2: Histogram of residuals from the DAME model (aggregating  $\epsilon_{ij}^t$  for  $1 \leq j < i \leq 97$  and  $1 \leq t \leq 32$ ).

As errors above seem closer to Laplacian than Normal distribution, we have tried an additional simulation based on Laplacian errors (while keeping other settings exactly the same as the simulation in Section 3.1 with medium correlation ( $\kappa = 2$ ), to examine the robustness of the DAME model to such error distribution misspecification. We find that if the errors are generated from Laplacian, our model performance is very similar to the normal error case. Therefore, our model seems to be robust when the errors are from Laplacian.

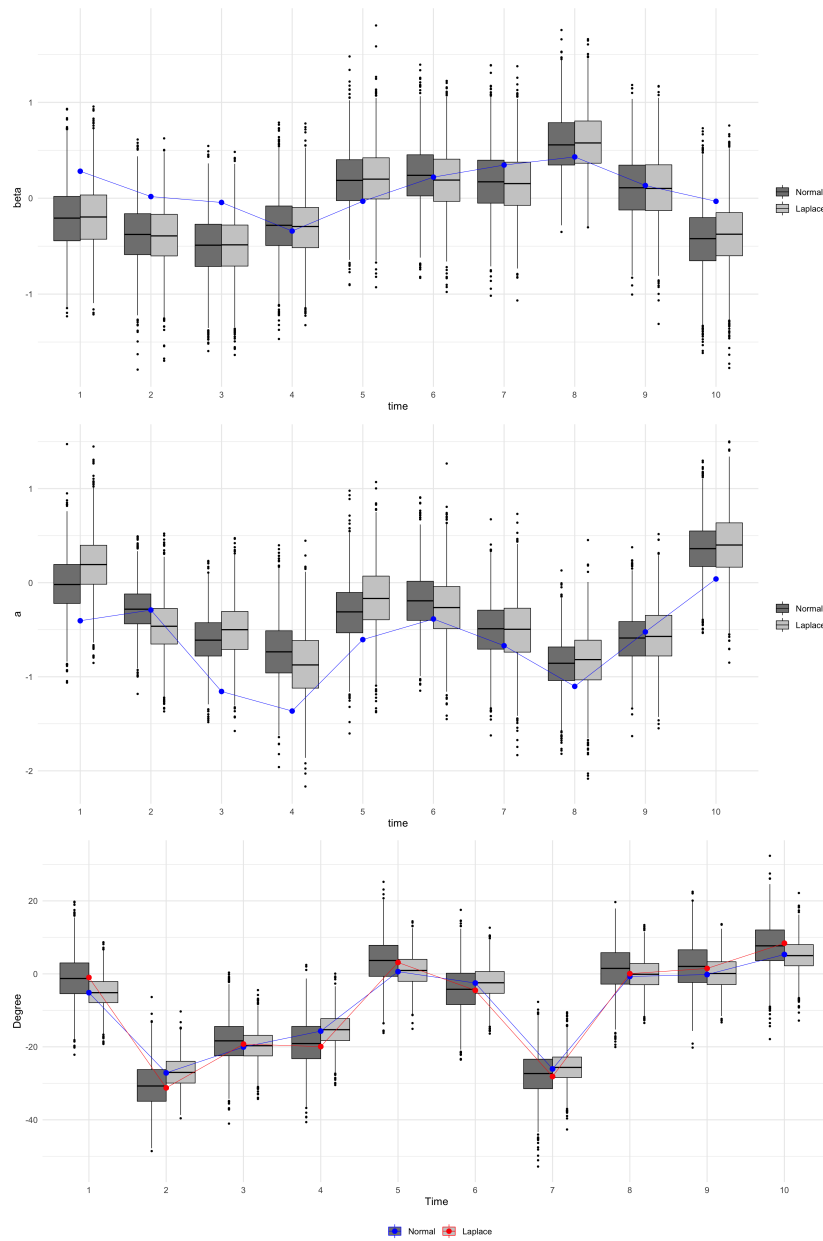


Figure 3: Boxplots of posterior samples of parameter estimates for the fixed effect (*upper*) and the additive effect for node 1 (*middle*), and posterior predictive degree statistics for node 1 (*lower*) shown with the dots representing true value of parameters or observed statistics. The observed degree depends on the error distribution so the true values are slightly different in the lower panel.

## G Posterior Summaries on GP Parameters

$\kappa$	$\kappa_{intercept}^\beta$	$\kappa_{\log(distance)}^\beta$	$\kappa_{polity}^\beta$	$\kappa_{alliance}^\beta$	$\kappa_{Trade/GDP}^\beta$	$\kappa_{language}^\beta$	$\kappa^\theta$	$\kappa_1^u$	$\kappa_2^u$
2.5%	27.883	1.876	53.448	1.432	136.582	1.352	3.567	9.251	0.762
25%	44.995	3.160	109.687	2.469	307.791	2.167	3.836	10.272	0.831
50%	60.641	4.301	162.852	3.214	486.600	2.797	3.989	10.804	0.866
mean	68.514	4.817	194.444	3.587	650.589	3.085	4.001	10.874	0.867
75%	82.561	5.761	234.342	4.262	786.030	3.638	4.156	11.452	0.904
97.5%	154.887	11.173	521.416	7.848	2076.781	6.614	4.482	12.693	0.971

Table 5: Posterior distribution of  $\kappa$ .

$\tau$	$\tau_{intercept}^\beta$	$\tau_{\log(distance)}^\beta$	$\tau_{polity}^\beta$	$\tau_{alliance}^\beta$	$\tau_{Trade/GDP}^\beta$	$\tau_{language}^\beta$	$\tau^\theta$	$\tau_1^u$	$\tau_2^u$
2.5%	403.820	0.161	0.087	0.978	0.091	0.420	29.211	6.870	4.061
25%	605.178	0.226	0.146	1.397	0.145	0.610	31.094	7.887	4.683
50%	780.451	0.281	0.194	1.720	0.196	0.748	32.208	8.520	50.046
mean	881.177	0.311	0.220	1.876	0.228	0.807	32.276	8.617	5.103
75%	1039.767	0.360	0.264	2.170	0.271	0.938	33.367	9.230	5.466
97.5%	1904.540	0.623	0.503	3.675	0.549	1.517	35.842	10.959	6.334

Table 6: Posterior distribution of  $\tau$ .

## H Posterior Predictive Checks

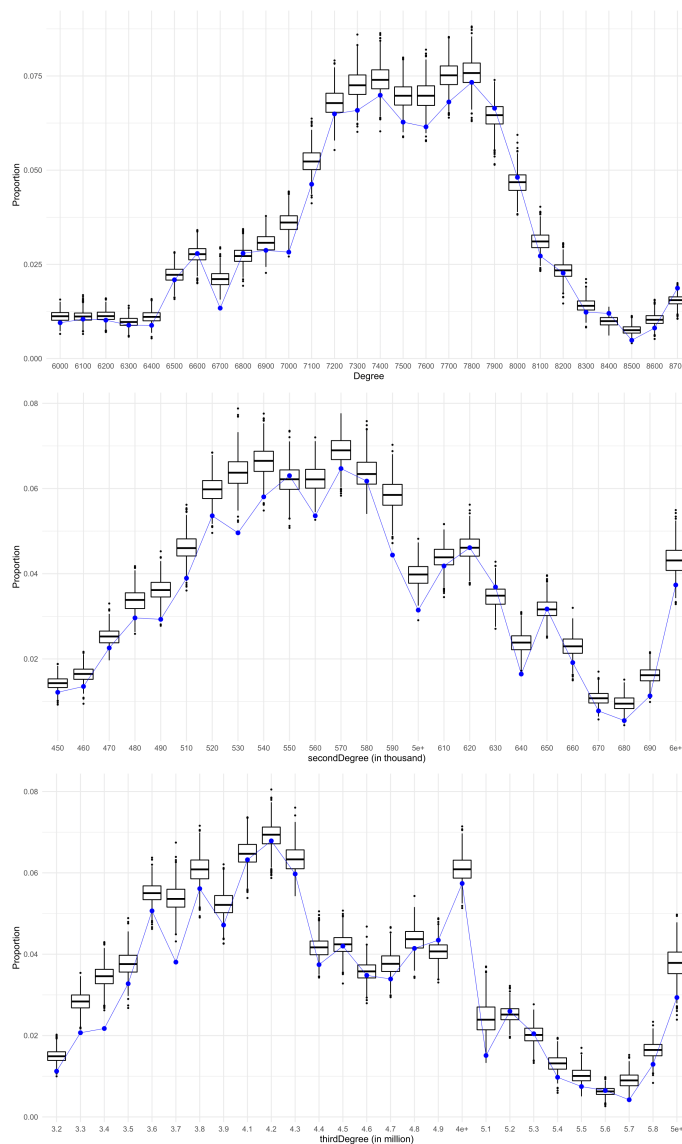


Figure 4: Posterior predictive plots of the overall degree distributions aggregating all nodes and timepoints: the first (*upper*), second (*middle*), and third moments (*lower*) shown with the dots representing observed statistics.

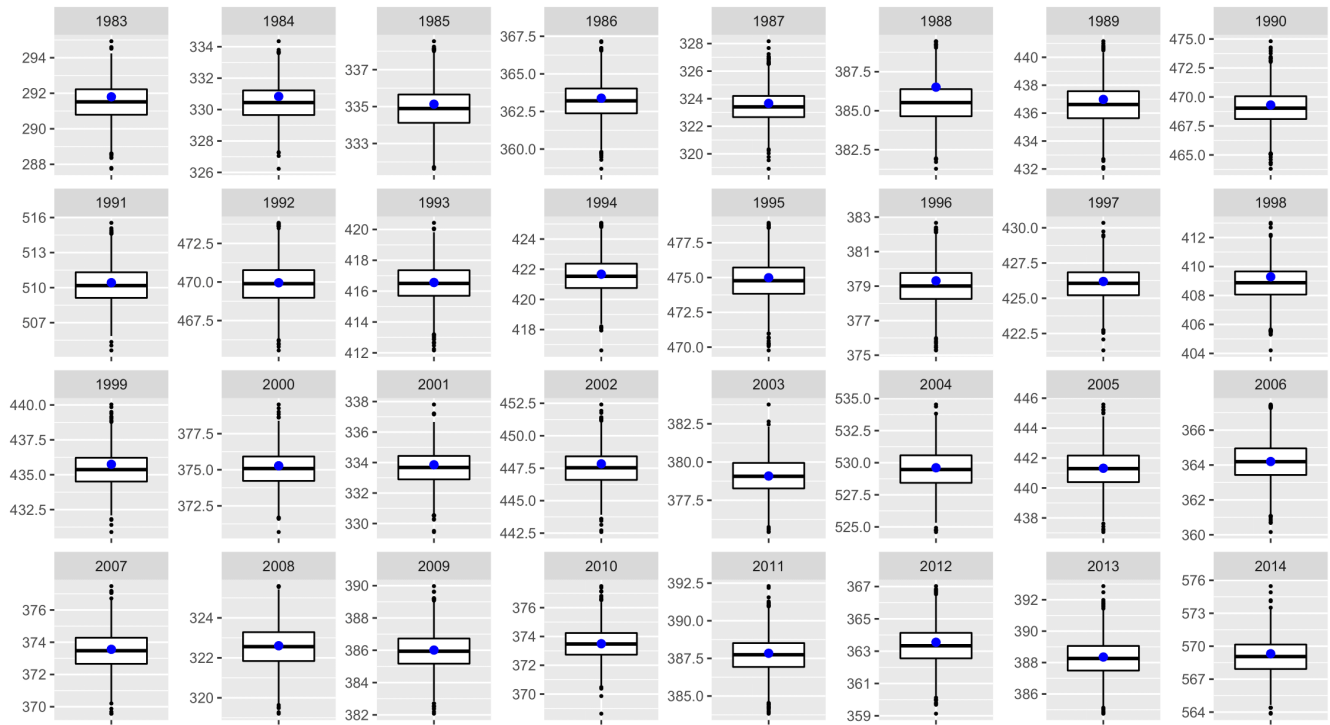


Figure 5: Posterior predictive plots based on transitivity statistics (defined as the sum of diagonals from third moments aggregating all nodes), shown with the dots representing the observed statistics.